INSTITUTE OF PHYSICS PUBLISHING SEMICONDUCTOR SCIENCE AND TECHNOLOGY

Semicond. Sci. Technol. **20** (2005) R65–R84 doi:10.1088/0268-1242/20/12/R02

TOPICAL REVIEW

Erbium in silicon

A J Kenyon

Department of Electronic and Electrical Engineering, University College London,
Torrington Place, London WC1E 7JE, UK

E-mail: t.kenyon@ee.ucl.ac.uk

Received 15 June 2005, in final form 4 August 2005
Published 9 November 2005
Online at stacks.iop.org/SST/20/R65

Abstract
The overlap of the principal luminescence band of the erbium ion with the low-loss optical transmission window of silica optical fibres, along with the drive for integration of photonics and silicon technology, has generated intense interest in doping silicon with erbium to produce a silicon-based optical source. Silicon is a poor photonic material due to its very short non-radiative lifetime and indirect band gap, but it has been hoped that the incorporation of optically active erbium ions into silicon will permit the development of silicon-based light sources that will interface with both CMOS technology and optical fibre communications. Some years into this activity, there have now been a wide range of experimental studies of material growth techniques, optical, physical and electrical properties, along with a considerable body of theoretical work dealing with the site of the erbium ion in silicon, along with activation and deactivation processes. This paper reviews the current state of what remains an active field, summarizing results from a range of studies conducted over the last few years, and points to further developments by considering the prospects for successful photonic integration of erbium and silicon.

1. Introduction

Microelectronics is now a mature technology that has undergone an astonishing rate of development from its inception in the 1960s and can now truly be said to dominate many aspects of modern life; for example, the current information revolution would not exist without the enormous degree of integration that is now commonplace. Nevertheless, the constant drive for ever more information at ever higher data rates is driving silicon microelectronics to its fundamental limits, and the search is on for technologies that will extend its reach, or supplant it altogether. Photonics, and particularly silicon photonics, is such a technology that has received an enormous amount of interest in recent years (see, for example, [1, 2]). The promise is that, by using light to transfer data between logic devices, very much higher data rates are achievable using photons instead of electrons. A particular and pressing concern for the next generation of silicon processor is the looming bottleneck caused by propagation delays and bandwidth limitations in on-chip electrical interconnects. As individual integrated devices become smaller, and hence the packing density larger, the total length of interconnects approaches several kilometres per chip. Add to this a decrease in dielectric thickness, and capacitance factors begin to severely limit the bandwidth of electrical interconnects. However, capacitance effects are absent in photonics, and hence losses are essentially independent of frequency. Various schemes and device geometries for silicon photonics have been proposed, including optical clock signal distribution, optical links between processors and direct interfacing with existing optical fibre systems for high-speed fibre-to-the-home communications. Each of these requires the development of a range of devices, including low-loss waveguides, photodetectors, modulators and electrically pumped optical sources; for true integration, these should be compatible with silicon, and in particular CMOS technology. To date, all of the required devices have been demonstrated in silicon, with one very important exception: an efficient optical source. Despite its pre-eminence in microelectronics, silicon has so far proved to be a poor material choice for optical sources, thanks to a number of factors: strong non-radiative recombination pathways result in a very short non-radiative

© 2005 IOP Publishing Ltd Printed in the UK

lifetime; it is an indirect band gap material, and there is a mismatch between its band edge luminescence at 1.1 μm and the requirement to operate at wavelengths around 1.55 μm for full compatibility with fibre optic communications systems. Although the problem of fast non-radiative channels can be mitigated, producing efficient emission [3, 4], the problem remains that this is in the wrong spectral range for use in telecommunications. Existing optoelectronic sources for use in the near infrared are therefore predominantly fabricated from direct band gap III–V semiconductors. Such materials offer the possibility of tuning both the band gap energy (and hence emission wavelength) and the lattice parameter of the active material over a wide range, and III–V materials are consequently a well-developed and mature technology. However, interfacing these materials with CMOS silicon drive electronics remains problematic and costly. No commercial silicon LED or laser exists, and the desire to produce such a device drives many research groups to investigate a range of possible solutions, including erbium doping of silicon.

Thus, the principal motivation behind the drive to incorporate erbium into silicon is to produce a CMOS-compatible optical source: an LED, an injection laser or an electrically pumped optical amplifier.

Existing fibre optic communication systems predominantly operate in the wavelength region between 1500 and 1600 nm, as this is the region in which the combined losses in silica fibres due to Rayleigh scattering, hydroxyl absorption and absorption due to the vibration of silicon–oxygen bonds are at a minimum. Wavelength division multiplexed (WDM) systems, particularly used for long-haul communications, manage to fit many parallel channels within this wavelength range, and the technology behind these systems is well developed and widely deployed. For full integration with such systems, silicon photonics must operate at these wavelengths. Doping silicon with erbium is a promising technique, as the trivalent erbium ion has an optical transition at 1535 nm, allowing access to telecommunications wavelengths. In optical fibre systems this is exploited in the erbium-doped fibre amplifier (EDFA), which uses population inversion in the erbium ion to produce optical amplification across a spectral range of some 50–60 nm. Assuming that the electronic properties of silicon are not significantly degraded by the incorporation of erbium and, furthermore, that the erbium can be introduced in an optically active state, this is a promising route to silicon-based optoelectronics. However, the simultaneous achievement of these two goals is far from trivial and has been the driving force behind a very active research community for a number of years.

However, erbium doping of silicon is not the only route to silicon optoelectronics currently receiving interest; the recent development of a CMOS-compatible silicon-based Raman laser operating in the 1.5 μm region is extremely significant [5]. Stimulated Raman scattering of pump photons in a silicon-on-insulator waveguide containing a reverse-biased p-i-n junction has been demonstrated to produce net gain of the order of 5.2 dB in a 4.8 cm length. Free-carrier absorption, which constitutes a serious loss mechanism in the near infrared, is suppressed by reverse biasing the junction, and hence sweeping carriers out of the waveguide. Nevertheless, such a device still relies on an external source of pump photons.

Two further techniques being actively investigated as a route to efficient near-infrared electroluminescence from silicon also deserve particular mention: the engineering of luminescent defects, and the formation of iron silicides. The former has received considerable attention since the announcement in 2001 by a group from the University of Surrey of an efficient silicon LED, which included as its active region a layer of luminescent dislocations in single-crystal silicon [6]. Standard CMOS processing was used to introduce dislocation loops using a boron implant; such loops generate carrier confinement and efficient band edge electroluminescence. This is of key importance for the production of integrated silicon photonics and could find application in on-chip and chip-to-chip communications. However, with a peak emission wavelength around 1150 nm at room temperature, this does not provide the silicon-based light source in the 1.5 μm region that is required for fibre communications. Nevertheless, the same group is investigating the feasibility of doping such a dislocation-engineered device with erbium to shift the luminescence band to telecommunications wavelengths [7]. Other defect technologies may also play a role here, however. Plastic deformation of crystalline silicon gives rise to a number of broad luminescence bands in the near infrared that are associated with dislocations in the silicon bulk [8–10]. The bands are conventionally labelled D1, D2, D3 and D4, and occur at wavelengths between 1250 nm and 1550 nm dependent on the nature of the crystal (p or n type, float zone or Czochralski material), the degree of deformation and the thermal history of the sample. Of these luminescence bands, the D1 line, which occurs at wavelengths around 1550 nm, is of particular technological interest. Although the D-bands all suffer from strong temperature quenching, much recent research has been directed to mediating this through the use of co-dopants, including erbium [11]. Recent work has demonstrated a silicon LED that produces D1 emission with a room-temperature efficiency of 0.1% [12]. Such a dramatic result was produced by reducing deep-level traps in the silicon by gettering and passivation.

The presence of D-band luminescence in the same region of the spectrum as that from the erbium ion can cause some confusion when assigning luminescence peaks in ion implanted material, and care must be taken to separate the two contributions [13]. Sobolev *et al* [14] have studied Er-implanted single-crystal Czochralski silicon and have observed simultaneous emission due to D1 and D2 dislocations (1.52 μm and 1.41 μm, respectively) and Er^{3+} ions (1.53 μm). Key to the assignment of emission bands is the observation that the D1 emission wavelength shows a dependence on temperature, shifting to longer wavelengths with increasing temperature. On the other hand, thanks to 4f shielding (more on this below), the position of the Er^{3+} $^4I_{13/2} \rightarrow {}^4I_{15/2}$ transition is insensitive to temperature. Work on iron silicides concentrates on understanding the luminescence of β-iron silicide, which has a luminescence band at 1550 nm [15], though again this suffers from strong temperature quenching and problems of compatibility with CMOS processing. Nevertheless, recent work concentrates on the contribution of impurities to increasing the luminescence yield from iron silicide [16].

The doping of semiconductors with erbium for photonic purposes is not a new field: the first report of an erbium-doped LED was in 1985 [17], but problems with achieving efficient room-temperature emission in erbium-doped silicon have proved a formidable challenge—both scientific and technological. A number of other semiconductor hosts, including GaAs, GaN and InP, have been investigated, but the technological imperative remains the achievement of 1.55 μm emission from a silicon-based material. Much of the work in the last two decades has therefore been focused on achieving a detailed understanding of excitation and de-excitation mechanisms of erbium in silicon in order to improve the material to the point where a device becomes feasible. Proof-of-principle devices have been demonstrated, reports of stimulated emission and the suggestion of gain have prompted debate and controversy, and the goal is tantalisingly close. However, as yet no commercial silicon-based device exists.

2. Erbium luminescence

Erbium is the 11th in the series of rare-earth elements in the sixth row of the periodic table and has the electronic configuration [Xe]$4f^{12}6s^2$. In common with other members of the series, erbium exhibits a number of intense and relatively narrow luminescence bands in the visible and near infrared. As an ion, erbium can exist in two oxidation states: Er^{2+} and Er^{3+}, with the former being encountered only rarely in semiconductors. The triply charged ion is formed by the loss of one 4f electron and both of the 6s, and it is this ion that is of most interest to the photonics community because of its radiative transitions in the near infrared around 1.53 μm. In this state, the 5s and 5p shells shield the incomplete 4f shell—as a result, luminescence from the ion is only weakly dependent on host. Erbium radiative transitions in solid hosts resemble those of the free ion (with some perturbation due to Stark splitting) and electron–phonon coupling is weak.

The intra-4f electronic transitions are parity forbidden in all rare-earth ions, but are partially allowed in low symmetry sites by crystal field interactions mixing odd- and even-parity wavefunctions and hence relaxing the dipole selection rules. In silicon, crystal field splittings tend to be the same for all sites for erbium ions, being around 200–300 cm^{-1}. As a result, luminescence lifetimes tend to be characteristically long in the absence of other non-radiative decay channels.

Energy levels in rare-earth ions are conventionally labelled according to their angular momentum and spin quantum numbers using term symbols such as $^4I_{13/2}$ or $^2F_{7/2}$. Here, the letter refers to the total orbital angular momentum of the ion obtained by combining the orbital angular momenta of the individual electrons in the ion according to the Clebsch–Gordan series. Under this scheme, S denotes an orbital angular momentum (L) of 0, P of 1, D of 2 and so on. I denotes an L of 6. The left superscript is the number of possible orientations of the total spin of the ion, given as $2S + 1$, where S is the total spin of the ion. The right subscript gives the total angular momentum of the ion and is determined using the Russell–Saunders coupling scheme [18].

Figure 1 shows the splitting of the $4f^{11}$ electronic energy levels of the Er^{3+} ion, illustrating the effect of electron–electron interactions and spin–orbit splitting. The ground state has

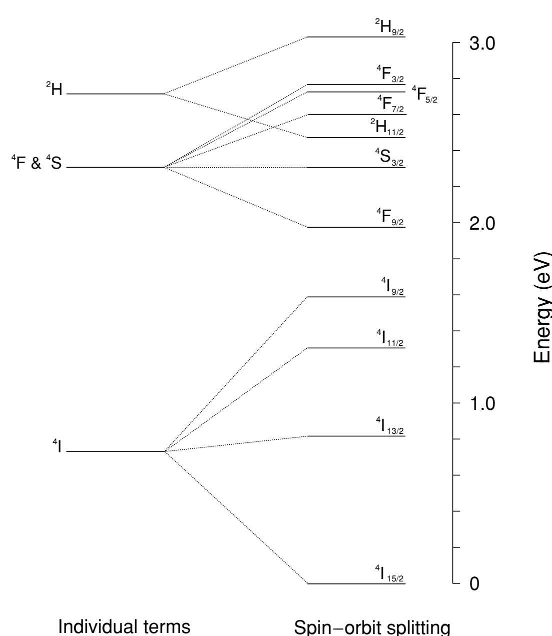

Figure 1. The splitting of the $4f^{11}$ electronic energy levels of the Er^{3+} ion, illustrating the effect of electron–electron interactions and spin–orbit splitting.

a configuration of ^4I, which splits into 9/2, 11/2, 13/2 and 15/2 terms due to the interaction between the electron's spin and its orbital angular momentum. The transition from the first excited state ($^4I_{13/2}$) to the ground state is responsible for the strong emission band around 1.55 μm. The lifetime of the $^4I_{13/2}$ state is long (up to 14 ms in an amorphous silica host, though this can be considerably reduced by non-radiative processes such as ion–ion interactions or Auger coupling with a semiconductor host), and hence this is often referred to as the metastable state. Absorption bands around 1480 nm, 980 nm, 800 nm and 520 nm correspond to transitions from the ground state to the top of the $^4I_{13/2}$, $^4I_{11/2}$, $^4I_{9/2}$ and $^4S_{3/2}$ manifolds, respectively. Other radiative transitions exist that yield luminescence in the visible region (for this reason, erbium found application as a component in phosphors well before it came to the attention of the silicon photonics community), but these are suppressed in silicon and are of little importance for telecommunications applications.

Stark splitting due to the crystal field of the host lifts the degeneracy of the erbium 4f energy levels, producing Γ_6, Γ_7 and Γ_8 Stark levels that give rise to multiplets in the low-temperature luminescence spectrum. For the special case of a cubic symmetry environment, Stark splitting of the $^4I_{15/2}$ ground state gives rise to five levels, whereas lower symmetry environments result in an eight-fold split [19]. At temperatures approaching room temperature, Stark splitting is the major source of luminescence broadening. Notwithstanding the above, the 5s and 5p shielding of the localized 4f orbitals means that the influence of the external crystal field is very much weaker than spin–orbit coupling.

A slight note of caution should be sounded here. Conventionally, theoretical descriptions of the electronic configuration of the Er^{3+} ion employ the so-called 'frozen 4f' approximation, which regards the 4f orbitals as totally screened by the 5s and 5p orbitals. In this scheme, any

interaction of the 4f orbitals with the valence electrons of the host is ignored [20]. This is generally a reasonable approximation that explains the relative insensitivity of erbium luminescence to host material, but there are suggestions that it is not necessarily always an accurate picture. Theoretical studies that allowed erbium 4f orbitals to be valence states, along with studies of chemisorption of erbium onto silicon surfaces, have suggested that the energies of the 4f electrons may be raised by the interaction with the silicon host [21], and photoemission experiments have demonstrated hybridization of the erbium 4f electrons with silicon valence electrons [22]. Local density approximation calculations published in more recent theoretical work have refined the treatment of the erbium orbitals in silicon by explicitly including terms to describe the strong localization of the 4f electrons [23] whilst still allowing some degree of hybridization. Such studies predict the existence of a number of states in the silicon band gap related to Er 4f levels. Although the energies of these levels do not match closely with experimental measurements, qualitative agreement is good. However, more seriously, any theoretical treatment that regards the 4f electrons as an isolated core shell cannot explain the crystal field splitting of the 4f levels that is seen in high-resolution low-temperature spectra of erbium in silicon. Nevertheless, it should be borne in mind that, although such studies provide valuable and interesting information, interactions between erbium 4f electrons and the valence electrons of the host are likely to be effects that are of secondary importance—in most situations, the frozen 4f approximation is a perfectly adequate working model.

Rare-earth ions are prone to ion–ion interactions and erbium is no exception. Coulombic interaction between neighbouring ions can efficiently transfer excitation from an initially excited ion to one in the ground state (energy migration), between two excited ions to leave one in the ground state and one in a higher lying state (co-operative upconversion), or from an ion in a high-lying state to promote a second from the ground state to the first excited state (cross relaxation). Such interactions depend upon dipole–dipole interactions that scale as $1/r^6$, r being the ion–ion separation, and hence are strongly dependent on erbium concentration. In addition, rare-earth ions are prone to aggregation in solid hosts. Beyond a critical concentration, ions cluster together to form aggregates that can be macroscopic in size, and in some cases even viewed using an optical microscope [24]. Such aggregates increase the probability of ion–ion interactions, and hence reduce luminescence efficiencies and lifetimes. Ion–ion interactions are a major problem in erbium-doped glasses, and whilst also important in silicon, they are partly mediated by the low solubility of erbium in silicon and are partly masked by other non-radiative de-excitation processes such as Auger interactions.

Low-temperature photoluminescence from erbium-doped silicon was first reported in the early 1980s [17, 25]. Up until that time, the focus of the photonics community in this area had been on the incorporation of rare-earth ions into glasses (for use in optical fibre devices such as the erbium-doped fibre amplifier (EDFA)) or III–V semiconductors. It soon became clear that room-temperature photoluminescence from erbium-doped silicon would present a considerable technical challenge, thanks to the presence of strong temperature quenching effects—in fact, room-temperature luminescence from erbium ions in silicon was not obtained until 1991 [26]. Early work demonstrated a reduction in photoluminescence from Er^{3+} in silicon of up to four orders of magnitude on warming from 15 K to room temperature, and it was only through extensive modification of the silicon host that this effect was reduced to the point at which room-temperature luminescence was feasible. Contrast this with the case of erbium in silica glass fibres in which temperature quenching is weak and the erbium-doped fibre amplifier is now a mature technology that operates efficiently at room temperature. However, many of the temperature quenching processes that occur in erbium-doped silicon are now relatively well understood, at least phenomenologically, and strategies are being adopted to minimize them, with the result that room-temperature photo- and electroluminescence are now a reality.

3. Incorporation of erbium into silicon

A number of techniques have been used to successfully introduce optically active erbium into silicon, including molecular beam epitaxy, sputtering, thermal diffusion, liquid phase epitaxy, chemical vapour deposition and, of course, ion implantation. In addition, a number of different forms of silicon have been investigated as potential host material—single crystal, polycrystalline, amorphous, nanocrystalline and porous. The last two may best be considered as quantum-confined systems, about which more later, whilst the former are bulk materials.

Of the preparation techniques mentioned for erbium-doped silicon, the majority of work has concentrated on ion implantation (see [24] for a review). This permits a high degree of control over the position of the implanted ions within the target material, but suffers from the disadvantage of introducing significant damage to the matrix. High-temperature annealing can recover the majority of this damage, but at the cost of producing aggregates of rare-earth ions or forming optically inactive silicides.

Molecular beam epitaxy (MBE) is an efficient way to grow erbium-doped silicon thin films without the problems associated with implantation damage, and as a result this technique has been widely employed [27–31]. It is particularly useful for the production of quantum-confined structures such as multilayer stacks and superlattices. Because of the very high quality of films that can be produced, it is sometimes possible to produce optically active erbium ions that occupy a single class of sites in the silicon host. This allows the physics of the silicon–erbium interaction to be studied to a level of detail that is not possible in implanted material.

A major problem facing researchers in this field is the relatively low solubility of erbium in crystalline silicon. A combination of ionic radii mismatch and the sp^3 bonding of the silicon host means that it is very difficult to incorporate high concentrations of erbium in crystalline silicon by equilibrium techniques such as thermal diffusion. Non-equilibrium methods, principally ion implantation, help somewhat, but even so, the practical concentration limit is around 3×10^{17} cm^{-3} [24]. Erbium concentrations of up to 10^{20} cm^{-3} have been achieved by epitaxial regrowth of erbium-doped amorphous silicon at temperatures below 900 °C [32]. Above

this temperature, epitaxy is not possible without greatly reducing the erbium concentration. However, in such highly doped material, only a small fraction of the erbium is optically active. Solubility remains an issue when other forms of silicon are used as hosts, though amorphous silicon can accommodate higher concentrations, and the use of co-dopants can help significantly. In all cases, erbium ions tend to aggregate together at high concentrations to form optically inactive clusters and silicides [27, 33].

Erbium complexes readily with a number of impurities in silicon—principally oxygen, and the maximum equilibrium concentration of erbium may be significantly increased by co-doping with impurities such as oxygen, carbon, nitrogen and fluorine [34–36]. Furthermore, the presence of such impurities strongly enhances erbium luminescence and reduces problematic temperature quenching effects. The 1991 report of room-temperature photoluminescence from erbium in silicon [26] relied on co-doping the silicon with oxygen, which produced a solvation shell around the erbium ions, reducing temperature quenching and at the same time promoting radiative transitions, increasing Er solubility and forming Er–O complexes that act as efficient electronic traps (more on this below). In order to ensure efficient electrical activation and a high percentage of optically active erbium ions, implantation of silicon with oxygen at a concentration an order of magnitude greater than that of erbium is necessary [37]. Annealing and structural studies have demonstrated that it is not sufficient merely to achieve the requisite concentrations of Er and O by implantation—it is also necessary to anneal the material to remove the implantation damage and to initiate the formation of Er–O clusters. Such clusters have been shown to resemble erbium ions surrounded by a coordination shell of oxygen with six-fold coordination between erbium and oxygen. Temperatures in excess of 650 °C are required to promote the formation of these clusters, and studies have demonstrated an optimum annealing temperature of 900 °C [38]. This correlates with the formation of specific donor species at energies around $E_c - 150$ meV, which are though to be related to Er–O complexes, detailed below. Note that in the following sections, E_c refers to the energy of the bottom of the silicon conduction band and E_v to the energy of the top of the valence band.

Co-doping with carbon can also enhance erbium luminescence [36]; in this case, it is thought that interstitial carbon atoms alloy with the silicon host to form $Si_{1-x}C_x$ compounds [39]. However, temperature quenching is a greater problem in this material than in oxygen-doped silicon, with no photoluminescence observable at temperatures higher than 170 K. Carbon introduces shallow levels in the silicon band gap at E_c − 10–20 meV, similar to those seen in oxygen-doped, erbium-doped silicon, but also produces deeper trap levels in the range $E_c - 90$ meV to $E_c - 108$ meV, the position of which depends on carbon content. It is thought that this variation arises as a result of localized changes in the silicon band gap energy caused by alloying.

The interaction between fluorine and erbium also serves to enhance erbium luminescence, though the effect does not seem to be analogous to the formation of a solvation shell around the erbium ions as seen in Er:O material. *Ab initio* calculations have failed to identify the erbium–fluorine configuration in Er:F-doped silicon, though they did confirm the six-fold coordination in Er:O material [40]. The mechanism of the fluorine-related luminescence enhancement remains undetermined, though the experimental demonstration of the effect is unambiguous.

Implantation at high fluxes of erbium into silicon can amorphize the upper layers of silicon above the implanted region. Because erbium has a higher solubility in amorphous rather than crystalline silicon, erbium segregates preferentially into the amorphous layers. Thus, as the sample is progressively annealed and recrystallization of the upper layers proceeds from the bulk towards the surface, erbium is 'pushed' towards the upper layers. A peak in the erbium concentration profile forms at the moving interface between the crystalline and amorphous layers. The degree of segregation, and hence the magnitude of this peak, depends critically on the erbium solubility and diffusivity, along with the rate of recrystallization of the amorphous layers. The situation changes when oxygen is present at high concentrations as a co-dopant; the formation of oxygen solvation shells around erbium ions greatly reduces their diffusivity and hence impedes the segregation process.

Amorphous silicon is a promising host for erbium, thanks to the increased solubility of Er in a-Si and the ease of co-doping with other impurities to activate the 1.54 μm luminescence band. However, although luminescence from Er-doped a-Si was first reported in 1990 [41], the poor electrical characteristics of amorphous silicon and the presence of defect-mediated luminescence pathways [42] initially limited electroluminescence to low temperatures (77 K). The use of hydrogenated a-Si overcomes many of these problems [43, 44]. The influence of hydrogenation has been widely studied [45] and there have now been a number of reports of electroluminescence from erbium-doped hydrogenated amorphous silicon. Recent studies of carbon co-doped erbium-doped hydrogenated amorphous silicon have demonstrated an enhancement of erbium luminescence that is thought to be due to the reduction of temperature quenching mechanisms as a result of an increase in band gap energy [46, 47]. Significantly, the inclusion of carbon into amorphous silicon does not degrade the electronic properties of the host to the same degree as does oxygen doping.

In the special case of porous silicon, erbium may be introduced into the matrix by electrochemical migration. After initially electrochemically etching the silicon substrate to make it porous, the HF electrolyte can be replaced with a solution containing erbium ions (for example, $Er(NO_3)_3$ or $ErCl_3$ in alcohol) and the erbium diffused into the porous silicon by the application of an electric field. Optical activation of the erbium is achieved by oxidizing the porous silicon in an oxygen atmosphere at 800–1000 °C. Note once again the key role played by oxygen in activating the erbium luminescence; this is a recurring theme in this field. However, the fragile nature of the host can make activation of erbium in porous silicon problematic, as the use of high annealing temperatures can damage the porous silicon matrix. Moreover, capillary forces generated during drying can damage the nanowires that make up the surface of porous silicon. Capping the surface with a layer of silicon nitride can greatly reduce the detrimental effect of high temperatures on the fragile host [48].

In the mid-1990s, the affinity of erbium for oxygen in silicon was exploited by groups in Italy and The Netherlands who investigated semi-insulating polycrystalline silicon (SIPOS) as a potential host for luminescent erbium ions [49, 50]. This material consists of a mixture of silicon and silicon oxide phases, and can readily be produced by chemical vapour deposition. By changing the relative mix of precursor gases (usually SiH_4 and N_2O), oxygen concentration in the SIPOS films can be varied over a wide range, with silicon-rich silica being produced for silicon excesses in the region of 5–15 at%. SIPOS contains mixed phases of suboxides, and films can be deposited that show a gradation in stoichiometry from pure silicon to around 30 at% oxygen. Such material was originally developed as an electronic material for use in high-voltage devices, though its optical properties soon generated interest. When such material is doped with erbium, carrier-mediated excitation of 1.54 μm luminescence is possible.

A material closely related to SIPOS that has received particular attention over the last decade is that of silica containing nanoclusters of silicon (so-called 'silicon-rich silica') [51–54]. Whilst not strictly erbium-doped silicon (as the current evidence suggests that the erbium in this material lies predominantly within the silica host), this is nevertheless an important material, representing a system intermediate between erbium-doped silicon and erbium-doped silica. A particular advantage of this material is that the interaction between silicon nanoclusters and erbium ions serves to increase the effective excitation cross section of erbium by up to four orders of magnitude [55]. Significantly, optical gain has been reported in this material using a low-cost solution: a blue LED [56]. However, as is usual with reports of optical gain in silicon-related materials, these reports have been the source of some controversy. Nevertheless, a number of techniques have been used for the production of this material: ion implantation of thermal oxide, PECVD, co-sputtering and Er implantation of PECVD-grown oxide amongst them. More details of research into erbium-doped silicon-rich silica are given later in section 8: quantum confinement effects.

Recently, a novel form of erbium-doped silicon was reported by Kimura's and Polman's groups [57]. Self-assembled multilayers of Si:Er:O were formed by spin-coating a single-crystal Si (1 0 0) substrate with erbium chloride, then oxidizing the sample using rapid thermal oxidation. Remarkably, although erbium concentrations as high as 14 at% were achieved, the samples exhibited strong luminescence with narrow linewidths and luminescence lifetimes around 200 μs. Excitation was possible either by direct excitation, or by the generation of photocarriers in the silicon layers. The self-assembly exhibited by this system makes it a very exciting potential photonic material.

4. The electronic states of erbium in silicon

In principle, erbium can be incorporated into silicon at either a substitutional or an interstitial site, though in practice the interstitial site is strongly preferred. This is not surprising, as the bonding mismatch between the ionic rare earth and the covalent semiconductor, along with differences in atomic radii, imply that the interstitial site will be more stable than the substitutional. In the case of the interstitial site, erbium will readily complex with nearby interstitial oxygen atoms, with the experimental evidence overwhelmingly indicating that the Er–O species acts as a donor. In common with the majority of other solid hosts, erbium exists in the 3+ oxidation state in silicon. There is some speculation that it is the presence of impurities with which the erbium can complex that favours the 3+ oxidation state over the 2+ [40].

Recent studies have demonstrated that the presence of oxygen can in fact change the erbium site from substitutional to interstitial [58]; following an initial implantation of erbium into single-crystal silicon, erbium is predominantly in the substitutional site, but a second implantation of oxygen drives the formation of Er–O complexes and the erbium becomes interstitial. Density functional calculations by Citrin *et al* [59] further suggest that the formation of Er point defects in oxygen-poor silicon is energetically improbable and that the preferred configuration is extended erbium silicide platelets. In these calculations, the energy of an erbium ion in the tetrahedral interstitial site is some 4.6 eV higher than that of the Er_3Si_5 phase. They postulate that the low energy of the extended defects arises because they allow for Er–Er metallic bonding, thus overcoming the problems associated with placing a metal ion in a covalent matrix. The calculations are supported by the observation by transmission electron microscopy of monolayers of erbium silicide precipitates in MBE-grown silicon containing very low levels of oxygen impurities.

Erbium is also implicated in the formation of shallow thermal donors in silicon. It is thought that the introduction of an erbium ion into the silicon matrix causes a local distortion of the lattice that can in turn stimulate the formation of thermal donors by acting as a trap site for oxygen atoms [60].

The above matches well with experimental evidence, which shows that not only does erbium act predominantly as a donor in silicon, but also the degree of donor behaviour correlates with the oxygen content of the matrix—a higher oxygen content results in a higher concentration of donors. Comparisons of float zone ($[O] = 1 \times 10^{16}$ cm^{-3}) and Czochralski (oxygen-rich: $[O] = 1 \times 10^{18}$ cm^{-3}) hosts confirm that erbium donor concentration in the latter is around one order of magnitude greater than in the former. Furthermore, if the initially oxygen-rich Czochralski material is further enriched by co-implantation with oxygen to achieve a peak oxygen concentration of 8×10^{19} cm^{-3}, the erbium donor concentration increases by a factor of 30 [61]. Results from the same study clearly demonstrate that the electrical activity of erbium in silicon is limited by the availability of oxygen. The optimum conditions appear to be those in which each erbium ion is coordinated with six nearest-neighbour oxygen atoms [37].

The situation is further complicated by the observation that the electrical activity of erbium-implanted Czochralski silicon is determined by several types of donor [62–64]: reference [64] employed Hall effect measurements to identify four of these as interstitial oxygen aggregates coordinated with intrinsic defects, and three types of Er–O complexes (labelled Er1, Er2 and Er3). Depending on the annealing temperatures employed, different mixes of these donor centres can be present. The oxygen aggregate/intrinsic defect states are shallow donors ($E_c - 20$ meV to $E_c - 40$ meV) that appear

rapidly after relatively low temperature anneals ($T \approx 700$ °C). At intermediate annealing temperatures (700–900 °C), such species are accompanied by two Er–O-related donors, at $E_c - 70$ meV (Er1) and $E_c - 120$ meV (Er2), respectively. However, annealing at temperatures in excess of 900 °C removes the $E_c - 120$ meV species and produces a new donor at $E_c - 150$ meV (Er3), also associated with Er–O complexes. This centre becomes the dominant one at such high temperature anneals and is strongly implicated in the carrier-mediated excitation of optically active erbium. There is also the suggestion of a further donor at $E_c - 100$ meV associated with erbium, though possibly not related to Er–O.

Studies of the electrical properties of erbium-implanted FZ silicon, detailed in the same reports, showed that in the absence of oxygen as a co-dopant, the dominant donor was a deep level at $E_c - 200$ meV. In previous studies, this has been assigned to Er-related trap levels (i.e. no involvement of oxygen) [65]. However, co-doping with oxygen produced the same levels referred to above, at $E_c - 70$ meV, $E_c - 120$ meV and $E_c - 150$ meV, confirming their assignment to Er–O complexes. Reference [62] further identifies a shallow donor at $E_c - 10$ meV present in samples implanted only with erbium; co-implantation with oxygen or sulphur produces deeper levels that correspond to those studied in [63, 64]. Photoluminescence studies allowed an assignment of this centre to erbium in a site of cubic symmetry. A further shallow centre was identified in the same study at $E_c - 14$ meV, which was assigned to an Er–O complex. Deep level transient spectroscopy (DLTS) measurements on material grown by MBE have also identified a deep level in p-type silicon at $E_c - 380$ meV, which appears to be associated with Er–O complexes [66]. High-resolution DLTS studies of erbium-implanted Czochralski silicon have further demonstrated the formation of an erbium-associated state at $E_c - 130$ meV [67]. DLTS and capacitance–voltage studies of liquid phase epitaxially grown erbium-doped silicon detected levels at $E_c - 200$ meV and $E_c - 390$ meV that correlated with the presence of optically active erbium [68, 69]. If the above picture seems confusing, it should be borne in mind that DLTS measurements are capable of a far higher accuracy than are Hall studies. The latter produce indicative results that suggest the presence of multiple donor states. By far, the most significant donor level from the perspective of optical activity is that found at $E_c - 150$ meV.

Implantation of impurity-free silicon with erbium introduces levels at $E_c - 200$ meV, $E_c - 260$ meV, $E_c - 340$ meV and $E_c - 510$ meV [36], all of which disappear when oxygen or other impurities are introduced; in the case of oxygen doping and high-temperature annealing, the familiar $E_c - 150$ meV donor state is formed. As an aside, it has been suggested that the $E_c - 150$ meV is related to the hybridization of erbium 5d orbitals with the silicon conduction band [70], but the majority of evidence implies that it is related to the formation of Er–O donor complexes. Nevertheless, it should be noted that this study concluded that, although the $E_c - 150$ meV level clearly plays a key role in activating erbium luminescence, only a very small fraction of the erbium ions form such a level—typically less than 1% of the total. The remaining ions introduce shallower levels that do not appear to participate in the luminescence mechanism.

As outlined earlier, similar erbium–impurity complexes can be formed by co-doping Si:Er with fluorine or carbon, and results have demonstrated increased erbium solubility, enhanced photoluminescence and weak temperature quenching in such co-doped material [36, 71] compared to erbium-doped silicon. Although the very shallow levels around $E_c - 10$–20 meV seen in Er:Si:O are also induced by these other dopants, the positions of the deeper levels are changed, with carbon doping producing levels in the range of $E_c - 90$ meV to $E_c - 108$ meV.

Furthermore, the environment seen by erbium in n-type silicon is different from that in p-type, and the latter exhibits higher photoluminescence intensities. In part, this is due to the donor nature of erbium in silicon, so that Er-doped p-type material simultaneously includes both donors and acceptors. It is therefore possible to produce p–n junctions by implanting p-type Si with erbium. Studies of non-radiative de-excitation processes of erbium in p-type and n-type material have yielded activation energies of 45 meV and 20 meV, respectively [72]. Such values are significant, as the B acceptor level in silicon is at $E_v + 45$ meV, the P donor level is at $E_c - 45$ meV and the oxygen aggregate level mentioned in the previous section is at $E_c - 20$ meV. These results strongly suggest, therefore, that de-excitation in n-type material proceeds via a shallow donor state that is absent in p-type silicon.

A puzzling result comes from DLTS and photoluminescence studies of erbium-doped silicon grown by sublimation MBE [60]. Despite strong photoluminescence from erbium, the deep level at $E_c - 150$ meV that has been linked with excitation of optically active Er^{3+} could not be detected. This suggests that different excitation pathways exist in this material and may imply therefore that multiple excitation pathways may exist in implanted silicon.

Table 1 summarizes the current picture of electronic states in erbium-doped silicon.

5. Site symmetry of erbium in silicon

The symmetry of the optically active erbium site in silicon remains somewhat controversial and clearly varies according to the presence and the chemical nature of impurities. Early photoluminescence studies by Przybylinska *et al* generated a confusing picture of more than 100 distinct emission lines from erbium in silicon, which were attributed to an array of different sites, including erbium–oxygen complexes, erbium-defect centres and isolated erbium ions at a range of sites of different symmetry [19, 73]. Moreover, because only a proportion of erbium in silicon is optically active, results from experimental and theoretical structural studies should be treated with some caution, as it may not always be the optically active erbium centre that is revealed.

Because erbium complexes readily with impurities, principally oxygen, and it is these impurity-related species that are most strongly implicated in the luminescence mechanisms, it is the symmetry of the various erbium–oxygen complexes that has received the most attention in recent years. Currently, there are three generic models for the Er–O species: tetrahedral interstitial (T_i-O), tetrahedral substitutional (T_s-O), and hexagonal interstitial (H_i-O) [74]. The substitutional site is thought to be unstable, as outlined previously, and

Table 1. Electronic states in Er-doped Si.

Energy (meV)	Assignment	Notes	References
$E_c - 10$	Er		[62]
$E_c - 14$	Er–O		[62]
$E_c - 10$–20	Er–C		[39]
$E_c - 20$–40	O defect		[64]
$E_c - 45$	P		[72]
$E_c - 70$	Er–O	Er1	[64]
$E_c - 90$–108	Er–C		[39]
$E_c - 100$	Er?		[64]
$E_c - 120$	Er–O	Er2: anneals out at 900 °C	[64]
$E_c - 130$	Er–O?		[67]
$E_c - 150$	Er–O	Er3: dominant after high-T anneal	[36, 64, 70]
$E_c - 200$	Er defect	Disappears in the presence of O	[36, 65, 69]
$E_c - 260$	Er defect	Disappears in the presence of O	[36]
$E_c - 340$	Er defect	Disappears in the presence of O	[36]
$E_c - 380$	Er–O	Only in p-type Si	[66]
$E_c - 390$	Er–O	In LPE Er:Si	[69]
$E_c - 510$	Er defect		[36]
$E_v + 45$	B		[72]

Table 2. Typical values of key parameters for Er in crystalline silicon.

Parameter	Symbol	Value	References
Electron–hole excitation cross section	σ_{eh}	3×10^{-15} cm^2	[72]
Impact excitation cross section	σ_{impact}	6×10^{-17} cm^2	[106, 102]
Direct excitation cross section (Er:SiO_2) @ 1535 nm	σ_{opt}	2.7×10^{-20} cm^2	[94]
Radiative lifetime	τ_{rad}	0.5–2 ms	[72, 103]
Backtransfer activation energy	E_{BT}	150 meV	[36, 64, 70]
Backtransfer rate (room temperature)	W_{BT}	1.7×10^6 s^{-1}	[94]
Backtransfer rate (15 K)	W_{BT}	0	[94]
Auger activation energy (p-type Si)	E_A	45 meV	[72]
Auger activation energy (n-type Si)	E_A	20 meV	[72]
Auger quenching rate (room temperature)	W_A	1.7×10^3 s^{-1}	[94]
Auger quenching rate (15 K)	W_A	0	[94]
Auger quenching constant	C_A	5×10^{-13} cm^3 s^{-1}	[72, 90]

both Rutherford backscattering and electron paramagnetic resonance (EPR) measurements have confirmed that only the two interstitial centres are commonly seen, with the proportion of erbium in substitutional sites being less than 5% [58, 75]. Bear in mind, however, that it is likely that the centres measured by EPR are not necessarily those that are optically active. Analysis of the fine structure of erbium luminescence in silicon suggests that the optically active species is a cubic centre within which the erbium ion sees a tetrahedral crystal field [19].

Ab initio theoretical studies by Wan *et al* indicated that the binding energy of erbium in pure silicon is positive, but the addition of oxygen makes this negative (−12.96 eV for interstitial erbium coordinated with six oxygen atoms at a tetrahedral site—T_i + O) [21], enhancing the otherwise poor solubility of erbium. The lowering is partly due to the fact that the binding energy of oxygen in silicon is negative (−11.99 eV), but the remainder of the lowering comes from the erbium–oxygen interaction.

Early EXAFS studies suggested that erbium in oxygen-rich Czochralski silicon coordinates with 6 nearest-neighbour oxygen atoms, while in FZ silicon each Er ion coordinates with 12 Si atoms [76], producing a site that should be optically inactive. Such an observation is surprising and suggests that the species being measured may in fact be an extended precipitate—perhaps a silicate, rather than a point defect. Such a view is supported by recent theoretical work from Jones' group in Exeter [77] that proposes the formation of $ErSi_2$ precipitates in FZ material that, on co-doping with oxygen, readily oxidize to optically inactive $Er_2Si_2O_7$ aggregates.

Recent EXAFS results from a study of MBE-grown and implanted material suggest an H_i-O site with an Er–O separation of 2.24 Å, an Er–Si separation of 3.6 Å and an Er–O–Si bond angle of 135° [74]. Contrast this with figures from the theoretical study by Wan *et al* [21] that produced separations of Er–O = 2.18 Å and Er–Si = 2.60 Å for the H_i + O configuration, and Er–O = 2.18 Å and Er–Si = 3.86 Å for the substitutional T_s + O configuration. It is suggested that the discrepancy in Er–Si bond length may be explained by considering an erbium ion in a hexagonal interstitial site in the middle of a V_6 hexavacancy decorated with oxygen [78]. Such hexavacancies are highly stable and can readily be induced by ion implantation. In this scheme, a V_6 centre with an overall symmetry of D_{3d} contains six oxygen atoms, which are isolated from each other by intermediate silicon atoms, and a single erbium ion placed at an H_i site. Because the interaction between the oxygen atoms is minimized by this configuration, they interact strongly with erbium and silicon atoms.

Related theoretical work by Ishii and Komukai investigated the symmetry point groups of various different possible configurations of six-fold coordinated Er–O clusters

in silicon [79, 80]. Using molecular orbital calculations, the effect of distorting the ErO_6 octahedron by selectively shortening one, two or three Er–O bonds to produce species with symmetries of C_{4v}, C_{2v} and C_{3v}, respectively, was investigated. It was found that the preferred site has C_{4v} symmetry, corresponding to an octahedron in which one Er–O bond has been reduced in length by around 0.1 Å.

Raffa and Ballone [81] applied density functional calculations to analyse the distortion of the silicon network caused by the inclusion of erbium ions coordinated with progressively higher numbers of oxygen atoms. For ErO_n complexes with $n \leqslant 6$, the equilibrium local Er–O coordination was found to have low symmetry—in fact, a significant conclusion of this study was that the symmetry was poorly defined, with the clearest trend being towards the formation of an isotropic solvation shell of oxygen atoms around the central erbium ion. The interstitial position of the erbium ion in the silicon matrix is confirmed by [81], which reports the variation in the energy difference between the substitutional and interstitial sites as a function of Er–O coordination number. On increasing coordination from two-fold to six-fold, ΔE increases from 0 to around 3.5 eV. First-principles calculations by Hashimoto *et al* [82] also suggest that the interstitial site is 2.84 eV more stable than the substitutional one for six-fold Er–O coordination.

One of the most compelling pieces of experimental evidence of the tetrahedral interstitial site comes from emission channelling studies of erbium-doped silicon [83]. This is an elegant technique in which the radioactive decay of ^{167}Tm to ^{167}Er produces electrons with a range of energies in the tens to hundreds of keV region depending on the decay pathway. Measurement of the angular distribution of the emitted electrons with respect to the crystal axes of the silicon host produces channelling patterns from which the location of the erbium ions can be inferred. Such studies indicate the localization of Er^{3+} on tetrahedral interstitial sites in both float zone and Czochralski silicon, and a strong interaction between erbium and oxygen in Czochralski material.

Very recent theoretical work by the Exeter group [77] involving density functional calculations on a range of Er and Er–O point defects, along with $ErSi_2$ and Er_2O_3, confirms the preferred tetrahedral interstitial site for erbium. They propose that the substitutional site introduces deep levels that would not be able to excite the erbium 4f levels. Interestingly, their results indicate an Er–O binding energy of around 1 eV for erbium–oxygen coordination numbers up to 6, suggesting the formation of extended Er–O complexes. Their results also have important implications for understanding diffusion of erbium in silicon. They found that the diffusion of an erbium ion from one tetrahedral interstitial position to the next proceeds via a hexagonal interstitial state, with an energy barrier in the region of 1.9 eV. This suggests that erbium diffuses relatively easily in silicon, and after annealing at 900 °C (a standard step to remove implantation damage), erbium readily complexes with impurities—principally oxygen. They further demonstrate that neither of the simple erbium point defects—substitutional or interstitial—can be optically active, as both have electronic states too deep in the silicon band gap to produce 4f emission. The optically active centre must therefore be associated with erbium–impurity complexes.

Hydrogen can also play a role in determining the symmetry of the erbium site: results from hydrogenation studies of erbium and oxygen co-doped silicon have suggested that the presence of hydrogen can stabilize the cubic Er centre and increase the erbium photoluminescence intensity with respect to non-hydrogen doped material containing a high concentration of cubic centres [84].

Luminescence studies have suggested that only a fraction of the erbium ions within silicon are optically active, and figures ranging between 1% and 10% have been suggested in different cases [19, 36], reinforcing the point that structural studies should be interpreted with some caution when attempting to determine the local environment of luminescent erbium ions. Recent work by Vinh *et al* has suggested that the site symmetry for the *optically active* erbium centre in silicon grown by sublimation MBE (SMBE) is C_{2v} [85]. Evidence comes from a detailed set of measurements of the Zeeman effect on luminescence from the principal erbium centre, Er1. Previous attempts to measure the Zeeman effect on erbium in silicon have been unsuccessful due to the inhomogeneous nature of the Er photoluminescence bands around 1.5 μm, though there are reports of narrow luminescence lines in other MBE-grown material [39]. However, the precise control afforded by the SMBE technique allowed high-quality Si/Si:Er superlattices containing erbium ions in very precisely defined environments to be deposited, and hence the erbium emission spectrum was reduced to a small number of very sharp lines [86]. The principal luminescence line exhibited a Zeeman effect that suggested C_{2v} symmetry, which it was suggested arose from the distortion of a tetrahedrally coordinated erbium ion. This is a significant result, as it implies that it is at least in some cases possible to produce a single optically active erbium centre, which considerably increases the likelihood of the successful realization of Er:Si photonic devices.

In the case of erbium-doped amorphous silicon, investigations of the local environment of the optically active erbium ions in oxygen-doped hydrogenated amorphous silicon have demonstrated that the luminescent ions are found within Er–O quantum dots [87]. The most likely configuration of these centres is generally thought to be six-fold tetrahedral coordination of the erbium ion with surrounding oxygen ions in C_{3v} symmetry [88] and an Er–O separation around 2.27 Å [75]. The size of these dots has been estimated to be around that of the unit cell of Er_2O_3 (1.05 nm). Evidence for this comes from emission Mössbauer spectroscopy, which demonstrates that the optimal ratio of erbium to oxygen in hydrogenated amorphous silicon is around 10:1—a similar result to that achieved for crystalline silicon.

6. Optical excitation and de-excitation mechanisms

In principle, two channels exist for optical excitation of erbium ions in a silicon host: direct photon absorption, and carrier-mediated excitation. In practice, the former process is rather unlikely, thanks to a combination of the high absorption coefficient of silicon at the wavelengths generally used for optical excitation and the rather small absorption cross section of erbium; hence, carrier-mediated excitation dominates [89], and hence most of the following concentrates on this.

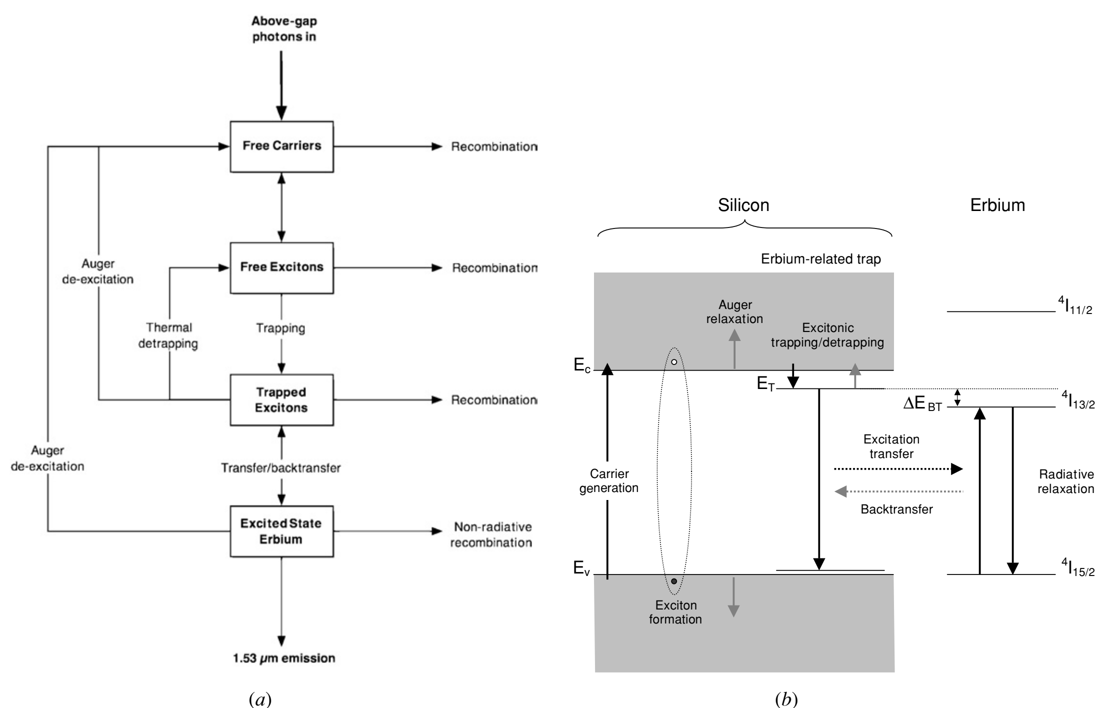

Figure 2. (*a*) The flow of energy in the excitation process, showing the steps required to produce free carriers, free excitons, trapped excitons and excited-state erbium ions. (*b*) The conventional energy-band diagram of the same processes, showing the relationship between the silicon band gap, the erbium-related trap level and the erbium ion. Processes leading to 1.53 μm emission are denoted using black arrows; loss mechanisms by grey.

Figure 2(*a*) outlines the flow of energy in the excitation process, showing the steps required to produce free carriers, free excitons, trapped excitons and excited-state erbium ions. Figure 2(*b*) illustrates the conventional schematic energy-band diagram of the same processes, showing the relationship between the silicon band gap, the $E_c - 150$ meV trap level and the erbium ion. Processes leading to 1.53 μm emission are denoted using black arrows; loss mechanisms by grey. Details of the individual steps are given below.

6.1. Excitation

Carrier-mediated excitation of erbium in silicon is a complex process that involves a number of steps, including several competing Auger interactions [90]. The starting point is the photogeneration, or direct injection in the case of electroluminescence, of carrier pairs, which readily form free excitons that have a number of relaxation pathways open to them: dissociation into free carriers, radiative or non-radiative relaxation, or trapping at deep levels. Note that band-to-band carrier recombination in the silicon host is very unlikely to result in excitation of the erbium ion [89]. Measurements of the dynamics of erbium photoluminescence [91] show that, at 4 K, excitation of erbium ions in silicon can continue for up to 50 μs after the end of the excitation pulse. This is longer than the lifetime of free carriers in silicon (typically sub-10 μs for the doping levels used in these studies), and hence the result suggests that those optically generated carriers contributing to the excitation of erbium ions rapidly become localized at erbium-related trap sites; 50 μs may therefore represent the characteristic lifetime of trapped carriers [36], or else this may be an indication of carrier diffusion and trapping times. Nevertheless, following trapping, excitons may then transfer their energy to erbium ions located at the trap centres to excite them to the $^4I_{13/2}$ state, from which radiative relaxation gives emission at 1.53 μm.

Clearly, a vital prerequisite for erbium luminescence is the presence of erbium-related trap states that can efficiently capture free excitons. Because other deep-level traps can compete by trapping excitons or allowing electron–hole recombination, other impurity centres should be minimized in order to maximize erbium luminescence. Whilst the incorporation of the trivalent erbium ion into the covalent crystalline silicon matrix introduces a number of erbium-related trap levels into the band gap, the stabilization of these traps and the removal of competing deep-level states are facilitated by the presence of oxygen, carbon or fluorine, and by high-temperature annealing. Typically, following annealing at temperatures around 900 °C, the dominant trap state is that associated with Er–O complexes at $E_c - 150$ meV; deeper levels, such as the Er-defect states at $E_c - 200$ meV, $E_c - 260$ meV, $E_c - 340$ meV and $E_c - 510$ meV are removed by the formation of Er–O complexes, thus reducing the opportunity for carrier trapping at optically inactive erbium states or other impurity centres. As a result, in the absence of exciton–electron Auger recombination (important only at high injection regimes), free excitons are rapidly captured by the erbium-related centres to form bound excitons. As the interstitial Er–O state is a donor, the hole capture rate determines the kinetics of exciton trapping [92]. Assuming that the bound excitons do not recombine via other competing pathways, they can transfer their energy to erbium ions via an impurity Auger process.

The optical excitation processes may be described using the following rate equations (after [93, 94]). Firstly, the generation of free excitons by optical excitation is given by

$$\frac{\mathrm{d}n}{\mathrm{d}t} = \frac{\mathrm{d}p}{\mathrm{d}t} = \alpha\phi - \gamma np \quad (1)$$

and

$$\frac{\mathrm{d}n_{\mathrm{ex}}}{\mathrm{d}t} = \gamma np - \frac{n_{\mathrm{ex}}}{\tau_{\mathrm{ex}}}, \quad (2)$$

where n_{ex} is the concentration of excitons, γ is the exciton binding coefficient, n and p are the concentrations of optically generated electrons and holes, respectively, ϕ is the photon flux and τ_{ex} is the excitonic lifetime, taking into account radiative and non-radiative recombination. The non-radiative contributions include trapping at various impurity centres: optically active erbium, optically inactive erbium and other impurities.

Next, these photogenerated excitons are trapped at Er–O centres at a rate that depends on the concentrations of free excitons and erbium-related traps. Note that it is a prerequisite of excitonic trapping that the Er–O centres are electrically neutral. The migration of the excitonic energy to the erbium 4f electrons follows. The generation of excited-state erbium ions (N^*_{Er}) is then given by

$$\frac{\mathrm{d}N^*_{\mathrm{Er}}}{\mathrm{d}t} = c_{\mathrm{A}} n_{\mathrm{ex}} (N_{\mathrm{Er}} - N^*_{\mathrm{Er}}) - \frac{N^*_{\mathrm{Er}}}{\tau}. \quad (3)$$

Here, c_{A} is the carrier capture coefficient for erbium-related traps and τ is the observed luminescence lifetime of the erbium ions (i.e. that resulting from both radiative and non-radiative decays). Note that typical values for the radiative lifetime of erbium in crystalline silicon range between 500 μs and 2 ms [72, 103].

Rates for carrier trapping (W_{T}) and detrapping (W_{D}) at erbium-related centres are given as [94]

$$W_{\mathrm{T}} = \sigma_{\mathrm{T}} v N_{\mathrm{T}}, \quad (4)$$

$$W_{\mathrm{D}} = \sigma_{\mathrm{T}} v N_{\mathrm{T}} \exp\left(-\frac{E_{\mathrm{T}}}{kT}\right), \quad (5)$$

where σ_{T} is the trapping cross section, v is the carrier velocity and N_{T} is the population of traps. From this, a trapping cross section of 3×10^{-15} cm^2 has been obtained [94]. E_{T} is the trap energy, taken to be 150 meV, corresponding to the dominant Er–O trap state. Note the strong temperature dependence of the detrapping process.

At this point, a simplifying assumption can be made that the excitonic relaxation rates are very much faster than the decay rate of excited-state erbium ions. Figures quoted by Hamelin *et al* are 2×10^8 s^{-1} for the former and 1×10^3 s^{-1} for the latter [94], so this is likely to be a reasonable assumption. Under these conditions, it can be assumed that the exciton population reaches equilibrium on a time scale very much less than the lifetime of the excited Er ions, in which case the excitonic population is a function of the absorption coefficient of silicon (α), the pump photon flux (ϕ) and τ_{ex}.

$$n_{\mathrm{ex}} = \alpha\phi\tau_{\mathrm{ex}}. \quad (6)$$

A further simplification is to define an *effective* absorption cross section as

$$\sigma_{\mathrm{eff}} = \alpha c_{\mathrm{A}} \tau_{\mathrm{ex}}, \quad (7)$$

in which case, the population of excited-state erbium ions becomes

$$\frac{\mathrm{d}N^*_{\mathrm{Er}}}{\mathrm{d}t} = \sigma_{\mathrm{eff}}\phi(N_{\mathrm{Er}} - N^*_{\mathrm{Er}}) - \frac{N^*_{\mathrm{Er}}}{\tau}, \quad (8)$$

which, under steady-state conditions, gives

$$N^*_{\mathrm{Er}} = \frac{\sigma\phi\tau N_{\mathrm{Er}}}{\sigma\phi\tau + 1}. \quad (9)$$

From this, the intensity of the erbium photoluminescence is given by

$$I_{\mathrm{PL}} = \frac{N^*_{\mathrm{Er}}}{\tau_{\mathrm{rad}}}. \quad (10)$$

Priolo *et al* [72] defined three efficiencies for optical excitation of erbium in silicon: (i) the efficiency of excitation of erbium per carrier pair; (ii) the ratio of photons emitted from erbium ions to the number carrier pairs; (iii) the external quantum efficiency taking into account losses at the silicon/air interface. From measurements at 15 K of the excitation power dependence of the photoluminescence intensity, all three efficiencies were determined. It was found that the excitation efficiency (i) could be as high as 10% for low pump powers, falling to around 0.2% at powers of 200 mW (taking the quoted beam diameter of 1 mm gives an approximate power density of 2.5×10^5 W m^{-2}). The internal quantum efficiency (ii) was found to be very close to the excitation efficiency for low powers, but dropped to around 0.03% at a power of 200 mW (2.5×10^5 W m^{-2}). At all pump powers, the external quantum efficiency (iii) was almost two orders of magnitude lower than the internal efficiency, due to refractive index mismatch at the silicon–air interface. This result implies that, as expected, low temperatures reduce the importance of competitive decay pathways for electron–hole pairs and also that non-radiative decay processes can be suppressed by operating at low pump powers. However, the real significance of this result is that the measured efficiencies are orders of magnitude higher than for equivalent concentrations of erbium in silica. Compare the measured internal quantum efficiency of 10% for Er:Si with that calculated for Er:SiO_2 of 2.5×10^{-5}% [72].

From the measured efficiency, a cross section for the excitation of erbium ions by electron–hole pairs can be defined (after [72]):

$$\sigma_{\mathrm{eh}} = \frac{\eta_{\mathrm{i}}\tau_{\mathrm{rad}}}{\phi_{\mathrm{Er}}\tau}, \quad (11)$$

where η_{i} is the internal quantum efficiency and ϕ_{Er} is the areal density of erbium ions. Evaluating this cross section from the data given above produces a value of 3×10^{-15} cm^2, which is greater than the cross section for impact excitation using hot carriers (6×10^{-17} cm^2 [102, 106]) and seven orders of magnitude greater than the cross section for direct optical excitation of erbium in silica (10^{-21} cm^2 [95]). Nevertheless, it must be borne in mind that these efficiency figures are for low-temperature excitation, and the strong temperature dependence of the various quenching effects changes the picture significantly for room-temperature luminescence.

Excitation processes in amorphous silicon are generally the same as in crystalline silicon, with the added complication of a higher density of trap states with differences in their energy levels. The radiative lifetime of the $^4I_{13/2}$ Er^{3+} state

is shorter in amorphous silicon than in crystalline silicon [96]. Measurements by Bresler *et al* of the shortening of the erbium luminescence lifetime due to stimulated emission in an amorphous silicon thin film gave an estimate of the radiative lifetime as 100 μs—compare this with previously quoted radiative lifetimes in silicon of between 500 μs and 2 ms.

Recent studies have suggested the existence of a different excitation mechanism that does not require the formation of an erbium-related state in the silicon band gap [97]. Using far-infrared terahertz radiation (provided in this study by a free-electron laser), erbium ions can be excited directly into the $^4I_{11/2}$ second excited state by free carriers in the silicon conduction band. This opens up the possibility of obtaining luminescence from a much higher percentage of the erbium ions present in the silicon than is possible using conventional methods. The decay time of the erbium photoluminescence produced by this scheme is much longer than that from above-gap excitation—apparently in the range of tens of milliseconds. This suggests that mid-IR excitation samples a different population of erbium ions than does conventional excitation. Moreover, this excitation scheme also offers the possibility of overcoming the strong temperature quenching caused by the backtransfer process; although experiments showed strong temperature quenching, it is possible that this is due to photoluminescence quenching by low power mid-IR pulses.

It is possible for mid-IR photons to either dissociate excitons localized at erbium-related traps or release carriers trapped at other sites not associated with erbium. The former leads to a reduction in erbium photoluminescence yield and the latter leads to an increase. Both effects have been demonstrated by Gregorkiewicz's group in Amsterdam [98]. However, the mechanism proposed in [97] is qualitatively different from these schemes in that it does not require the trapping of excitons at erbium-related levels. Instead, free carriers in the conduction band are excited to higher lying levels in the same band that are resonant with one of the erbium 4f levels. Significantly, this mechanism populates the second excited state of the erbium ion, thereby producing a three-level system and opening up the possibility of true population inversion. The processes involved in the proposed mid-IR excitation mechanism are outlined in figure 3.

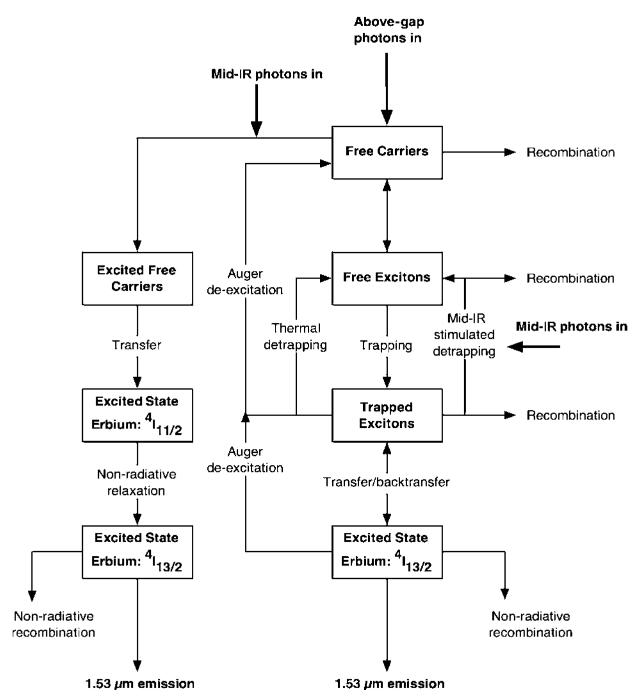

Figure 3. Processes involved in the mid-IR excitation mechanism described in [97].

Very recent results have suggested the existence of a further excitation mechanism in thin epitaxial erbium-doped silicon structures [99]. Photoluminescence excitation measurements indicate an anomalously strong signal from erbium when excited using photon energies less than that of the silicon band gap. Comparison of the PLE spectrum of excitons generated within the epitaxial layers with that of the erbium ions indicated that the sub-gap excitation of erbium does not involve the generation of excitons, and it is therefore postulated that the initial absorption step involves the promotion of an electron from the valence band directly into an erbium-related defect state. Recombination of the electron with the corresponding hole in the valence band produces the energy required to excite the erbium ion into the $^4I_{13/2}$ state, from which it can decay radiatively.

There is a further potential excitation mechanism that deserves mention at this point. The observation of a very slow component in the photoluminescence signal from erbium in silicon [100], with a characteristic lifetime in the region of 25 ms, is phenomenologically similar to the afterglow effect seen in phosphors. It has been proposed that this luminescence is produced by the thermal release from shallow traps of carriers that then become available to excite nearby erbium ions. Once again, this effect was studied using a mid-infrared free-electron laser to release the carriers from the shallow traps. Such a mechanism, whilst a potential limitation on the modulation speed of an electrically pumped erbium-doped silicon source, may nevertheless find application in optical memories.

Single-crystal silicon samples implanted with a thin buried layer of erbium can exhibit strong erbium photoluminescence when excited from the un-implanted side of the sample. Given a typical sample thickness of 500 μm and an implantation depth of less than 1 μm, this implies excitation of the Er^{3+} centres by carriers diffusing through the bulk material [101]. However, luminescence dynamics studies of this material have shown that the time taken for excitation to reach the erbium layer from the back face is very much longer than would be expected from a consideration of the carrier diffusion rate in bulk silicon. The authors propose that this is a result of the formation of a pn junction by the implanted erbium layer. Excitation cannot flow to the erbium until the junction potential is sufficiently reduced by accumulated charge.

6.2. De-excitation and Auger effects

The strong temperature quenching of erbium luminescence in crystalline silicon is attributed to rapid loss of excitation back to the silicon matrix. Because the excitonic binding energy is small and the dominant optically active erbium-related trap centre lies only 150 meV below the silicon

conduction band, thermal detrapping of the bound excitons to form free excitons occurs readily at temperatures above 130 K. Similarly, an efficient Coulombic backtransfer process operates between excited-state Er^{3+} ions and trapped excitons. For both processes, the small mismatch in energy between the forward (*excitation*) process and the reverse (*de-excitation*) is readily provided by phonons—hence the strong temperature dependence of luminescence. A further mechanism, which becomes important at high carrier concentrations, is that of Auger de-excitation through interaction with free carriers in the silicon matrix [102]. Free carriers can be optically generated (in the high flux regime) or may be introduced by thermal donors, doping (n- or p-type) and even by the presence of erbium, which is itself a donor. This process is highly temperature dependent and typically becomes important at temperatures greater than 30 K. Thao *et al* have demonstrated the importance of including two separate Auger de-excitation processes in modelling the luminescence of erbium in silicon: the Auger decay of bound excitons and excited-state erbium ions [90, 103]. A further possibility is the dissociation of free excitons into electrons and holes.

Auger quenching of excited-state erbium ions by free carriers can be described as (after [94])

$$W_A(T) = C_A N_D \left(1 + 2\exp\left(-\frac{E_D - E_f}{kT}\right)\right)^{-1}, \qquad (12)$$

where $W_A(T)$ is the temperature-dependent quenching rate, C_A is the Auger quenching coefficient, N_D is the donor concentration, E_D is the donor energy and E_f is the Fermi energy. C_A has been measured, under low photon fluxes to avoid the photogeneration of high concentrations of free carriers, as approximately 5×10^{-13} cm^3 s^{-1} [72]; note that this study suggested the presence of different Auger mechanisms in p- and n-type silicon. In the former, the activation energy for Auger quenching was found to coincide with the acceptor level of B in silicon (E_v + 45 meV), implying quenching of erbium luminescence by holes in the valence band. On the other hand, the activation energy for Auger quenching in n-type silicon was found to be 20 meV, which does not correspond to the energy of the P donor level (E_c − 45 meV). However, because erbium introduces a donor level at E_c − 20 meV, this was taken as evidence that the Auger interaction in n-type material is between excited-state erbium ions and electrons released by erbium donors. Note further that the same study determined that the Auger quenching coefficient for the interaction between erbium ions and *bound* excitons was two orders of magnitude smaller than that between erbium ions and free carriers.

Early studies by Suchocki and Langer [104] on the luminescence quenching of transition metal ions in CdF_2 by the free-electron Auger effect demonstrated an inverse relationship between luminescence decay time and free carrier concentration. They proposed that this should be the dominant Auger quenching effect in semiconductors. Extending this argument to erbium in silicon, the following relationship may be expected to hold:

$$\tau^{-1} = \frac{n}{n_0 \tau_{rad}}, \qquad (13)$$

τ being the luminescence decay time, n the free carrier concentration, τ_{rad} the radiative lifetime and n_0 given by

$$n_0 = 4\pi^{5/2} n_r^{5/2} \left[\frac{137 a_0 m_0}{m^*}\right]^{1/2} \lambda_0^{-7/2}, \qquad (14)$$

where n is the free carrier concentration, λ_0 is the emission wavelength, a_0 is the Bohr radius, n_r is the refractive index of the semiconductor host, τ_{rad} is the radiative lifetime, and m_0 and m^* are the electron rest mass and effective mass, respectively. From this relationship, the Auger coefficient can be defined as

$$C_A = \frac{1}{\tau_{rad} n_0}. \qquad (15)$$

Priolo *et al* have evaluated this for erbium in silicon [72] and obtained a value of 7×10^{-13} cm^3 s^{-1}, in good agreement with the measured value of 5×10^{-13} cm^3 s^{-1}. Independent measurements by Palm *et al* give a value of 1.4×10^{-12} cm^3 s^{-1} [90]. An important consequence of this relationship is that the decay lifetime can be tailored to a specific value by changing the free carrier concentration. Above a threshold value, the decay time will be reduced below the radiative lifetime. In the case of crystalline silicon, this critical concentration has been determined by Franzò *et al* [105] as 1×10^{15} cm^{-3}. Palm *et al* quote a value of 7.6×10^{14} cm^{-3}, which is in very good agreement [90].

Given a measurement of the Auger quenching coefficient, the Auger quenching cross section can be determined from

$$\sigma_A = \frac{C_A}{v}, \qquad (16)$$

where v is the thermal velocity of carriers. Priolo *et al* determined this to be approximately 5×10^{-20} cm^2 [72]. This is significant, as measurements of the cross section for impact excitation of erbium in electroluminescent devices give values around 6×10^{-17} cm^2 [106]. The three orders of magnitude difference requires some explanation, as the two processes should, on first inspection, be the reverse of each other. However, under impact excitation, electrons with sufficient energy can excite the erbium ion to higher lying electronic states, whereas the Auger de-excitation measured by monitoring 1.53 μm emission only occurs from the $^4I_{13/2}$ level. Thus, the impact excitation cross section is an effective cross section that is best considered as the integral of cross sections for a number of transitions from the $^4I_{15/2}$ ground state to higher lying levels.

Auger quenching of excitons through interactions with free carriers has been investigated by Palm *et al* and by Hangleiter and Häcker [90, 107], who demonstrated that Auger recombination in silicon is strongly enhanced by electron–hole correlation (i.e. the formation of excitons). An Auger quenching coefficient for this process was measured to be 1×10^{-10} cm^3 s^{-1}.

A study of excitation mechanisms [94] by probing backtransfer from erbium ions excited using 1.53 μm photons suggested that the probability of de-excitation of a given erbium ion by backtransfer to the silicon matrix in ion implanted material can be as high as 70%. Moreover, it was found that the backtransfer rate exceeds that of Auger quenching of Er luminescence by three orders of magnitude at room temperature (1.7×10^6 s^{-1}; cf 1.7×10^3 s^{-1}) and

that both rates are nearly zero at 15 K. However, the reported external quantum efficiency for generation of photocurrent from 1.5 μm illumination is of the order of 10^{-6} due to the small absorption cross section of erbium at this wavelength (2.7×10^{-20} cm^2) [94].

Table 2 summarizes typical values of key excitation and de-excitation parameters for erbium in silicon.

7. Electroluminescent devices

The ultimate goal of erbium-doped silicon photonics is the production of an electrically pumped light source that can be readily integrated into standard CMOS processing technology. Electroluminescence from an erbium-doped silicon p–n junction grown by molecular beam epitaxy was first reported in 1985 [17]. An erbium-doped p-type layer was grown onto an n-type substrate and 1.53 μm luminescence was seen under forward bias at 77 K. However, temperature quenching of the forward bias electroluminescence is similar to that seen for photoluminescence, and hence the signal can reduce by almost two orders of magnitude on warming the sample to room temperature. In order to overcome this temperature quenching due to the Auger effect, reverse biasing the junction excites erbium ions using hot electrons. In this case, room-temperature electroluminescence can be obtained, though the impact cross section is small, and hence the electroluminescence is low [102, 108]. However, the emission spectrum obtained in reverse bias is very different from the forward bias case. Low-temperature spectra from the latter typically consist of a number of sharp lines with full width half maxima around 1 nm; however, under reverse bias, erbium ions in SiO_x precipitates are excited and the corresponding luminescence spectra have linewidths of tens of nanometres [109]. In addition, the excitation of erbium ions under reverse bias by impact excitation does not require the presence of the customary $E_c - 150$ meV Er-related trap state, and it is thus thought that a larger proportion of erbium ions are excited than is the case for carrier-mediated photoluminescence [110].

The addition of a thin nonstoichiometric suboxide layer to the diode structure can serve to raise the average kinetic energy of electrons injected into the active region by imposing a barrier of around 300 meV [111]. An enhancement of a factor of around 2 was reported for electroluminescence from such a structure compared to a conventional diode with no suboxide layer.

As is the case for photoluminescence studies, the intensity of electroluminescence can be greatly increased by co-doping the active region with oxygen or fluorine [112]. Similar effects are thought to be responsible for this—increased solubility, stabilization of erbium–impurity complexes, reduction of temperature quenching.

It is instructive to consider in more detail the excitation and de-excitation processes that occur in an erbium-doped Si LED. Following the analysis of [110], a rate equation for Er in Si under electrical pumping can be written as

$$\frac{\mathrm{d}N_{\mathrm{Er}}^*}{\mathrm{d}t} = \sigma\frac{J}{q}(N_{\mathrm{Er}} - N_{\mathrm{Er}}^*) - \frac{N_{\mathrm{Er}}^*}{\tau}, \tag{17}$$

where σ is the cross section for impact excitation, J is the current density, q is the electronic charge and τ is the electroluminescence lifetime, taking into account non-radiative de-excitation. The steady-state solution yields

$$\frac{\mathrm{EL}}{\mathrm{EL_{max}}} = \frac{\sigma\tau\frac{J}{q}}{\sigma\tau\frac{J}{q}+1}. \tag{18}$$

The time evolution of EL is governed by the characteristic decay time τ on switch-off, whilst the rise time is governed by a factor dependent on the cross section and current density:

$$\mathrm{EL} \propto \mathrm{EL_{max}}\left[1 - \exp\left(-\left(\sigma\frac{J}{q} + \frac{1}{\tau}\right)t\right)\right]. \tag{19}$$

From independent measurements of the dependence of the electroluminescence intensity and rise time as a function of current density, it is possible to extract both σ and τ. Typical room-temperature values are $\sigma = 6 \times 10^{-17}$ cm^2 and $\tau = 100$ μs [102, 106]. However, an interesting feature of the electroluminescence is that the switch-off time is much less than the rise time—reference [110] quotes a value of 12 μs switch-off for a luminescence decay time of 100 μs. This seemingly contradictory result can be explained by considering the microscopic structure of the pn junction during operation of the diode. Under reverse bias, the optically active erbium ions within the depletion region are excited by hot carrier impact. In fact, the ions towards the edges of the depletion region are preferentially excited, as this is the region containing the most energetic carriers. However, when the field is removed, the depletion region shrinks rapidly (governed by carrier diffusion) and the excited-state erbium ions now find themselves in material containing a high concentration of free carriers (typically 10^{19} cm^3). Under these conditions, erbium luminescence is rapidly quenched by Auger interactions with the free carriers. Given the size of the Auger de-excitation cross section (10^{-12} cm^2), the erbium luminescence decay should be reduced to the nanosecond regime, allowing fast modulation of the LED. Reference [110] reports modulation speeds of up to 10 MHz. This is potentially significant, as the realization of high luminescence efficiency requires a long luminescence lifetime, whilst fast modulation requires τ to be short. These contradictory requirements may be reconciled if the luminescence lifetime is long during pumping and short at turn-off.

Despite the fact that the cross sections for the excitation of erbium in silicon by electron–hole recombination and impact by hot electrons are large (3×10^{-15} cm^2 and 6×10^{-17} cm^2, respectively) compared to the excitation cross section of erbium in silica (10^{-21} cm^2), strong temperature quenching effects reduce the luminescence yield from electroluminescent devices at room temperature. Moreover, despite the fact that $\sigma_{\mathrm{eh}} > \sigma_{\mathrm{impact}}$, impact excitation is more efficient in erbium-doped LEDs because the observed emission is from erbium ions within the depletion region, in which Auger interaction with free carriers is reduced. Direct measurements of the excitation cross section of Er in a forward-biased diode yield large values, typically in the region of 10^{-15} cm^2. However, under forward bias the erbium ions see a large population of free carriers, and hence Auger de-excitation is efficient and rapid, drastically reducing the electroluminescence efficiency. Thus, high-efficiency electroluminescence from erbium in silicon is best obtained under reverse bias.

Because carriers must have an energy greater than the energy of the $^4I_{13/2} \rightarrow {}^4I_{15/2}$ erbium transition (0.8 eV), there

is a region within the depletion region within which erbium ions cannot be excited by hot electron impact. Carriers are generated by tunnelling processes at the centre of the depletion region (i.e. around the pn junction) and are accelerated by the applied field towards the edges of the depletion region. Thus, the energies of the carriers at the centre of the depletion region are typically less than 0.8 eV, and as a result erbium ions in this region are 'dark'. In order to overcome this problem, an npn transistor structure may be used in which the collector–base junction is erbium doped. In this case, carriers are injected from the emitter, accelerated across the base by a reverse-biased collector–base junction and produce erbium luminescence by impact excitation. Because the carriers have acquired significant energy during their time in the base, there is no 'dark' region, and hence high-efficiency electroluminescence can be achieved [113].

8. Quantum confinement effects

The band structure of semiconductors is a result of short- and long-range interactions between the large number of atoms in a typical crystal, so it should come as no surprise that reducing the dimensions of a semiconductor crystal to the nanometre scale will extensively modify its electronic structure. When the critical dimension of semiconductor structures is smaller than the excitonic Bohr radius ($\sim$5 nm for silicon), quantum confinement effects due to the confinement of electrons in one, two or three dimensions become important. Confinement of carriers in real space causes their wavefunctions to spread out in momentum space, increasing the probability of radiative processes due to greater wavefunction overlap. Moreover, decreasing the size of the quantum well or quantum dot within which the carriers are confined increases the spacing between electronic energy levels, and hence the band gap energy increases. Changing the size of the quantum system thus allows the band gap energy, and hence luminescence wavelength, to be tailored to a specific application.

A caveat should be added at this point; as the degree of confinement increases (i.e. the dimensionality reduces or the size of the system becomes smaller), so too does the contribution of surface states. In the case of luminescent silicon nanoclusters smaller than 5 nm, the surface or interface atoms make up a sufficiently large proportion of the total that the presence of a single defect at the interface is thought to be sufficient to trap carriers and quench the luminescence [114]. Control of the quality of the interface is therefore a key requirement in order to achieve efficient luminescence from confined systems.

Nevertheless, because of the modification of their band structure, doping confined silicon systems with rare-earth ions can help to overcome some of the non-radiative de-excitation problems associated with bulk silicon. Quantum confinement effects also produce long carrier lifetimes and a high degree of localization in real space. This may both suppress the Auger backtransfer processes that limit luminescence efficiency in bulk silicon and increase the interaction probability between the confined carriers and the luminescent rare-earth ions.

Perhaps, the most widely studied confined silicon system is porous silicon, which arises as a result of electrochemical etching of single-crystal Si, producing silicon pillars or wires, which may be tens or hundreds of microns long but nanometres wide. First investigated as a photonic material by Canham in 1990 [115], porous silicon was initially of interest as a source of visible light. In porous silicon, photogenerated carriers are confined within the silicon pillars or wires, and this confinement greatly increases the efficiency of photo- and electroluminescence from silicon. Furthermore, the band gap of porous silicon may readily be controlled by varying the etch conditions, and therefore the porosity of the material. The peak luminescence wavelength may thus be varied by controlling the etch step, and as a result a number of electroluminescent devices have been made that emit in the visible region. However, porous silicon is not suitable for application in fibre optic communications, as confinement effects can only increase the band gap from its bulk value, and hence shift the band-to-band luminescence to shorter wavelengths. In common with bulk silicon, therefore, erbium doping is required to produce emission in the 1.5 μm region. Several groups have incorporated erbium into porous silicon by ion implantation, thermal diffusion or by electrochemical methods, to produce 1.5 μm sources based on silicon [116–119]. Photoluminescence excitation measurements have demonstrated a combination of direct optical excitation and carrier-mediated indirect excitation pathways from Er-doped porous silicon [120].

The etching process that generates porous silicon produces a host that is inherently oxygen-rich, which is favourable for erbium luminescence. Nevertheless, the photoluminescence intensity from erbium in porous silicon increases with post-diffusion activation temperature, reaching a maximum for anneals around 1100 °C. However, the conductivity of porous silicon falls exponentially with annealing temperature. Likewise, increasing both the thickness and the porosity of the porous layer (and therefore the degree of quantum confinement) reduces the conductivity. Care must therefore be taken when designing electroluminescent devices from erbium-doped porous silicon; an activation temperature of around 800 °C represents a compromise between luminescence efficiency and conductivity, and produces the most intense emission [121].

Electroluminescence studies of erbium-doped porous silicon indicate the existence of different luminescence mechanisms for the two biasing conditions—a similar result to that seen for bulk silicon Er-doped LEDs. Different temperature quenching effects are observed in forward and reverse biases, with very different activation energies. The implication is that there are at least two erbium-related trap levels in porous silicon [121]. Nevertheless, temperature quenching of erbium emission in porous silicon is less pronounced than in crystalline silicon, possibly due to the increased band gap and the lack of an extended crystalline lattice, though luminescence bandwidths are narrow: around 10 nm at room temperature. The luminescence lifetime of the 1.5 μm emission depends on temperature, being around 1 ms at 300 K; such temperature behaviour suggests that thermal quenching is a result of the thermalization of carriers localized at erbium-related trap levels [122].

A novel technique for the activation of erbium luminescence using porous silicon was recently reported, in which the porous material was produced by the growth of

silicon nanowires on a silicon substrate using $SiCl_4$. Erbium-doped silica was then deposited onto the wires using a sol–gel process. The thin silica layer allowed efficient electrical activation to be achieved, and coupling with the quantum-confined silicon nanowires produced high luminescence efficiencies [123]. Related studies on the synthesis of erbium-doped silicon nanowires without an oxide capping layer have enabled samples to be grown by chemical synthesis that consist of single-crystal silicon cores surrounded by polycrystalline erbium-doped layers. The presence of hydroxyl groups on the surface of the wires appears to quench the 1.5 μm erbium luminescence [124].

Work by Wang *et al* [125] has characterized the optical efficiency of different erbium sites in porous silicon. Comparing samples doped by immersion to those implanted with erbium, temperature quenching was much stronger in the latter, implying that the preferred site for efficient luminescence from erbium in porous silicon is at the surface of the pores rather than deeper in the bulk material. This may be due to the influence of oxide layers around the porous silicon nanowires.

A second class of confined silicon host is that of silicon nanocrystals in an amorphous silicon host, which may be produced by, for example, laser annealing of amorphous silicon [126]. In this system, confinement is produced by the crystalline–amorphous boundary [127, 128], and doping this material with rare-earth ions leads to enhanced rare-earth emission due to the same quantum confinement effects seen in porous silicon. Luminescence at 1.5 μm has been obtained from erbium incorporated into a ridge waveguide of nanocrystalline silicon, and stimulated emission with a pumping threshold of 10 MW cm^{-2} was reported. This is clearly a highly significant report, though there is some controversy over these results, and it has been frustratingly difficult to confirm this as representing real net optical gain—stimulated emission was measured by measuring output from a waveguide device as a function of excitation power dependency, but no gain has been measured. In common with porous silicon, erbium-doped microcrystalline silicon films exhibit much weaker temperature quenching effects than is the case for bulk silicon [129]. However, in this case it is thought that the erbium ions lie within the amorphous silicon, which, having a larger band gap energy than bulk silicon (1.6 eV compared to 1.1 eV at 300 K), suffers from backtransfer effects at higher temperatures than bulk silicon [130]. Studies of Stark splitting showing eight sharp lines in the emission spectrum of erbium in amorphous/nanocrystalline silicon films suggest that the optically active species is an octahedrally coordinated erbium ion in an ErO_6 complex [88].

By placing the erbium-doped silicon active layer within a microcavity, radiative transition probabilities may be greatly increased, and to exploit this effect devices have been constructed that consist of Fabry–Perot microcavities incorporating the active layer. This layer may be either amorphous or porous silicon [131–134], and confinement effects produced by resonating structures produce short luminescent lifetimes, allowing the high modulation rates required of sources based on erbium-doped silicon active layers.

One approach has been to fabricate structures of alternating layers of silicon and silica, thus forming Bragg reflector stacks surrounding a quarter-wavelength thick active erbium-doped layer, which may be erbium-doped silicon or erbium oxide [135]. Such systems are often referred to as silicon–silica superlattices [136–138]. Strong confinement produced by high-Q cavities can modify both the spectral linewidth and the luminescence lifetime of the erbium emission as well as enhancing emission intensity and directivity. Careful design of the microcavity can result in nearly 100% reflectivity in the stop band with a reflectivity minimum at the erbium emission wavelength of 1.54 μm.

In the case of porous silicon, multilayer structures can be fabricated by modulating the etching current during sample production. In this way, layers of alternating refractive index may be produced such that Bragg mirrors may be formed either side of a chosen active layer [133, 139]. Erbium can be introduced into the porous layers using electrochemical doping, or the layer may be implanted with erbium. As is the case for 'bulk' porous silicon, annealing in oxygen or nitrogen [121] activates the erbium luminescence. Such a structure produces enhancement and linewidth narrowing of erbium emission, though suffers from the drawback that emission from erbium incorporated in porous layers outside the active region (i.e. within the Bragg mirrors) cannot be suppressed. Recent reports have demonstrated Q factors around 1500 for erbium implanted into porous silicon microcavities [140]. Care must be taken in the design of the microcavity, as the oxidation/annealing step changes the density, and therefore the refractive index, of the porous layers. This results in a wavelength shift in the reflectivity spectrum of the cavity, which must be allowed for in order for the reflectivity minimum to overlap the erbium emission band after annealing.

The periodic nature of the Bragg cavity constitutes a photonic band gap structure, and therefore the erbium emission from within the cavity is both highly directional and enhanced. Emission through the Bragg stack can be up to 38 times more intense than that in-plane from the side of the sample and is concentrated into a 20° cone around the surface normal [133]. The ability to tailor the cavity structure also enables the emission peak to be centred in a wavelength region within which erbium emits only weakly. The luminescence enhancement produced by the cavity therefore compensates for the low yield at these wavelengths.

Extending the concept of placing the optically active rare-earth ions into a resonant cavity, Polman's group has investigated the effect of modifying the radiative transition rate of Er^{3+} in silica microcavities [141]. Cavities were formed either by producing erbium-doped silica thin films or by producing a highly monodisperse size-selected set of erbium-doped silica colloidal spheres with diameters in the range of 150–350 nm. In both cases, the radiative transition rate of the Er^{3+} 1.5 μm transition could be modified greatly by changing the refractive index of the ambient by placing the films or microspheres in contact with liquids having a range of refractive indices [142]. Modification of the decay rate occurs as a direct result of changes in the local density of states function surrounding the erbium ions.

A quantum-confined rare-earth doped material that has been attracting attention recently is erbium-doped silicon-rich silica. This material consists of silica doped with excess silicon in the form of nanometre-sized clusters and can be considered

as a three-dimensionally confined silicon system in which the confinement is produced by the silicon–silica boundary. The embedded silicon clusters may be either amorphous or crystalline, and because of quantum confinement effects, emit light in the visible and near-infrared region. Such material has been studied for some time as a promising candidate for light emission from silicon [143–145]. Photoluminescence efficiencies are low [146], as it is generally thought that even for nanoclusters as small as 2 nm in diameter, the silicon remains predominantly indirect-gap and non-radiative lifetimes remain short. However, when co-doped with rare-earth ions the situation is dramatically improved: intense rare-earth emission can be obtained, and doping with erbium allows access to the 1.5 μm spectral region.

Indirect excitation of erbium photoluminescence via coupling between the absorption bands of the silicon nanoclusters and erbium excited states has been demonstrated by a number of groups [51, 52, 147, 148]. Quantum confinement effects can be used to tailor the absorption band edge of the silicon nanoclusters and move it into the visible region [145]. Absorption of incident photons then proceeds via the broad-band absorption of the nanoclusters, producing confined excitons. This step is followed by rapid excitation exchange to the rare-earth ions and consequent luminescence at 1.5 μm from the erbium metastable state. Luminescence from the silicon nanoclusters is in competition to that from the rare-earth ion, though by using a sufficiently high rare-earth concentration silicon nanocluster luminescence can be effectively quenched. It is likely that the transfer takes place via a dipole–dipole interaction leading to population of (as yet unspecified) higher exited states of the erbium ion that feed into the $^4I_{13/2}$ metastable state via rapid phonon-assisted decay. Studies of material produced by both ion implantation and PECVD [55, 148] have shown that the presence of silicon nanoclusters can increase the effective absorption cross section of erbium in silica by four orders of magnitude to around 7×10^{-17} cm^2.

A recurring problem in studies of silicon nanoclusters is the difficulty of producing a monodisperse size distribution of clusters; given that the cluster dimensions at least partially control the optical properties, any distribution of cluster sizes will result in a corresponding distribution of cluster band gaps. However, work by Zacharias' group has demonstrated the possibility of precise control of cluster size and size distribution [149]. By growing superlattices of alternating layers of silicon and silicon dioxide by reactive evaporation, then initiating phase separation by annealing, nanocrystals with a diameter determined by the thickness of the silicon layer can be formed. Very tight size distributions are achieved by this technique. Studies by the same group of erbium-doped superlattices demonstrate efficient coupling between nanocrystals and erbium ions [150].

Because the initial absorption of pump photons is by the broad-band absorbing silicon nanoclusters, the constraints on pump wavelength are considerably relaxed. Instead of requiring a narrow-band pump source tuned to one of the Er^{3+} absorption bands, broad-band sources can be used. Pumping of Er^{3+} emission in silicon-rich silica using a commercial camera flashgun has been demonstrated [151]. This opens up the possibility of cheap flashlamp-pumped erbium-doped optoelectronic components. Furthermore, Shin's group has demonstrated optical gain at 1.53 μm in a ridge waveguide structure of silica doped with silicon nanoclusters [151]. Significantly, the excitation source was a commercial blue LED. Despite reported problems with precise control of the material parameters, this is an extremely significant result, as it opens up the possibility of a broad-band pumped erbium-doped gain elements and possibly a silicon-based laser. A subject that caused some controversy in the field was the report of an increase in the erbium-stimulated emission cross section of a factor of 10–50. This appeared to run contrary to the observed erbium luminescence lifetime, which is very similar to that of Er in silica. Very recent work has reported signal enhancement as in similar device and quantifies the spectroscopic properties of the rare-earth ions coupled to nanoclusters—the measurements suggested that the absorption cross section of the Er ions is close to that seen for Er in silica, and it is only the effective excitation cross section that shows enhancement [152]. It would be wrong to say, however, that this settles the question of the apparent enhancement of the erbium emission cross section, as this has been reported by more than one group. Some reconciliation of the different results is required here. Nevertheless, current optically pumped waveguides do not address the need for an electrically pumped source and can be thought primarily as a route to miniature low-cost planar analogues of the erbium-doped fibre amplifier.

To address the need for an electrically pumped source, electroluminescence has been achieved from an erbium-doped silicon-rich silica [153] and silicon nanolayer/silica films [154]. In the case of the former, thin layers of erbium-doped silicon-rich silica were deposited by magnetron sputtering onto silicon substrates. Ohmic contacts were diffused into the bottom of the substrate and gold contacts evaporated onto the top surface of the samples. Electroluminescence results showed lower threshold and increased efficiency over a similarly produced erbium-doped silicon device. In the case of the silicon nanolayer samples, a thin layer of silicon ($d < 4.0$ nm) was deposited by magnetron sputtering onto a film of erbium-doped silica grown on a silicon substrate (both n+ and p were used) and a top contact of gold used for electrical connection. The thin silicon layer constituted a confined system from which excitation could be transferred to the erbium ions in the silica layer in an analogous way to that seen in erbium-doped SiO_x. The intensity of the electroluminescence was found to be strongly dependent on the thickness of the nanometre-scale silicon layer. In 2003, ST Microelectronics reported electroluminescence at 1.54 μm with an external efficiency of 10% from MOS devices containing silicon nanoclusters and erbium in the oxide layer [155]. It remains to be seen if such devices will be fully commercially exploited, as lifetime problems due to the high fields applied across the active layers remain a serious issue. Nevertheless, this is a result that is scientifically important.

Similar electroluminescence studies have been performed on thin rare-earth doped silica layers incorporated into MOS devices [156]. Both erbium and terbium have been employed as the optically active rare-earth ion and have been implanted into 50 nm SiO_2 layers. Erbium ions are excited by hot electrons as a result of Fowler–Nordheim tunnelling, which

produces electrons with average energies in excess of 5 eV. In the case of the erbium-doped device, an enhancement of ~7 times was seen in the EL from the MOS structure when compared to that from an erbium-doped pn diode. Internal efficiencies of $>4 \times 10^{-5}$ and impact excitation cross sections of 1×10^{-15} cm^2 were reported.

9. Conclusions

A great deal of progress has been made in recent years towards understanding the physics of the erbium-doped silicon system. Despite initial results that suggested that luminescence could only be achieved at cryogenic temperatures, it is now possible to obtain room-temperature photo- and electroluminescence. Excitation and de-excitation mechanisms are now relatively well understood at the phenomenological level, and the complexities of the various electronic states of erbium in silicon are beginning to be unravelled. Moreover, the exploitation of quantum effects to enhance cross sections and increase luminescence yields has brought the goal of silicon-based optoelectronics tantalisingly close. Nevertheless, there remain a number of questions to be answered and problems to be overcome before erbium-doped silicon photonics can become a viable technology. The wide range of excitation and de-excitation processes involved in erbium luminescence in silicon makes this a very complex system, and in order to obtain high-efficiency electroluminescence a number of competing processes must be understood and controlled. This presents formidable scientific and technological challenges. From a scientific point of view, it is fair to say that a detailed understanding of all of the processes involved in light emission from erbium in silicon is still elusive. Amongst the technological issues to be considered are the minimization of free-carrier absorption, the reduction of temperature quenching effects, the inclusion of a high percentage of optically active erbium in silicon, the control of the electronic states of erbium in silicon and monolithic integration of erbium-based sources with other photonic components. In addition, there remains some significant controversy surrounding the small number of reports of optical gain in erbium-doped silicon. All measurements in the literature are indirect—superlinear relationships between photoluminescence and excitation power, and amplified spontaneous emission measurements using variable excitation lengths (the 'variable stripe length method'), for example. The ultimate proof of useful gain in this material remains the demonstration of real net signal enhancement in a waveguide, and to date such measurements remain ambiguous and the goal of an erbium-doped silicon amplifier is as elusive as ever. Nevertheless, even the suggestion of optical gain from this material represents a tantalising hope, and since the potential benefits from its realization are so great, this is an area of research that remains extremely active. Of course, erbium-doped silicon is not the only promising material system, but it still remains the brightest hope for CMOS-compatible sources operating at telecommunications wavelengths.

References

[1] Pavesi L and Lockwood D J 2004 *Silicon Photonics* (Berlin: Springer)
[2] Pavesi L 2003 *J. Phys.: Condens. Matter* **15** R1169
[3] Trupke T, Zhao J H, Wang A H, Corkish R and Green M A 2003 *Appl. Phys. Lett.* **82** 2996
[4] Green M A, Zhao J H, Wang A H, Reece P J and Gal M 2001 *Nature* **412** 805
[5] Rong H, Liu A, Jones R, Cohen O, Hak D, Nicolaescu R, Fang A and Paniccia M 2005 *Nature* **433** 292
[6] Ng W L, Lourenço M A, Gwilliam R M, Ledaln S, Shao G and Homewood K P 2001 *Nature* **410** 192
[7] Lourenco M A, Milosavljevic M, Galata S, Siddiqui M, Shao G, Gwilliam R M and Homewood K P 2005 *Vacuum* **78** 551
[8] Fitzgerald E A, Currie M T, Samavedam S B, Langdo T A, Taraschi G, Yang V, Leitz C W and Bulsara M T 1991 *Phys. Status Solidi* a **171** 227
[9] Higgs V, Lightowlers E C, Fitzgerald E A, Xie Y H and Silverman P J 1993 *J. Appl. Phys.* **73** 1952
[10] Blumenau A T, Jones R, Oberg S, Briddon P R and Frauenheim T 2001 *Phys. Rev. Lett.* **87** 187404
[11] Kenyon A J, Steinman E A, Pitt C W, Hole D E and Vdovin V I 2003 *J. Phys.: Condens. Matter* **15** S2843
[12] Kveder V, Badylevich M, Schroter W, Seibt M, Steinman E and Izotov A 2005 *Phys. Status Solidi* a **202** 901
[13] Vernon-Parry K D, Evans-Freeman J H, Hawkins I D, Dawson P and Peaker A R 2001 *J. Appl. Phys.* **89** 2715
[14] Sobolev N A, Gusev O B, Shek E I, Vdovin V I, Yugova T G and Emel'yanov A M 1999 *J. Lumin.* **80** 357
[15] Schuller B, Carius R, Lenk S and Mantl S 2001 *Opt. Mater.* **17** 121
[16] Terai Y and Maeda Y 2005 *Opt. Mater.* **27** 925
[17] Ennen H, Pomrenke G, Axmann A, Eisele K, Haydl W and Schneider J 1985 *Appl. Phys. Lett.* **46** 381
[18] Atkins P W 1983 *Physical Chemistry* 2nd edn (Oxford: Oxford University Press)
[19] Przybylinska H, Jantsch W, Suprun-Belevitch Yu, Stepikhova M, Palmetshofer L, Hendorfer G, Kozanecki A, Wilson R J and Sealy B J 1996 *Phys. Rev.* B **54** 2532
[20] DeLerue C and Lannoo M 1991 *Phys. Rev. Lett.* **67** 3006
[21] Wan J, Ling Y, Sun Q and Wang X 1998 *Phys. Rev.* B **58** 10415
[22] Rossi G 1987 *Surf. Sci. Rep.* **7** 1
[23] Fu Y, Huang Z, Wang X and Ye L 2003 *J. Phys.: Condens. Matter* **15** 1437
[24] Polman A 1997 *J. Appl. Phys.* **82** 1
[25] Ennen H, Schneider J, Pomrenke G and Axmann A 1983 *Appl. Phys. Lett.* **43** 943
[26] Michel J, Benton J L, Ferrante R F, Jacobson D C, Eaglesham D J, Fitzgerald E A, Xie Y-H, Poate J M and Kimerling L C 1991 *J. Appl. Phys.* **70** 2672
[27] Efeoglu H *et al* 1993 *Semicond. Sci. Technol.* **8** 236
[28] Sobolev N A *et al* 2005 *Phys. Solid State* **47** 113
[29] Kuznetsov V P, Rubtsova R A, Shabanov V N, Kasatkin A P, Sedova S V, Maksimov G A, Krasil'nik Z F and Demidov E V 2005 *Phys. Solid State* **47** 102
[30] Scalese S, Franzò G, Mirabella S, Re M, Terrasi A, Priolo F, Rimini E, Spinella C and Carnera A 2000 *J. Appl. Phys.* **88** 4091
[31] Buyanova I A, Chen W M, Pozina G, Ni W X, Hansson G V and Monemar B 1998 *J. Vac. Sci. Technol.* B **16** 1732
[32] Polman A, Custer J S, Snoeks E and van den Hoven G N 1993 *Appl. Phys. Lett.* **62** 507
[33] Eaglesham D J, Michel J, Fitzgerald E A, Jacobson D C, Poate J M, Benton J L, Polman A, Xie Y-H and Kimerling L C 1993 *Appl. Phys. Lett.* **58** 2797
[34] Carey J D, Barklie R C, Donegan J F, Priolo F, Franzò G and Coffa S 1998 *J. Lumin.* **80** 297
[35] Liu P, Zhang J P, Wilson R J, Curello G, Rao S S and Hemment P L F 1995 *Appl. Phys. Lett.* **66** 3158
[36] Priolo F, Franzò G, Coffa S, Polman A, Libertino S, Barklie R and Carey D 1995 *J. Appl. Phys.* **78** 3874
[37] Coffa S, Priolo F, Franzò G, Bellani V, Carnera A and Spinella C 1993 *Phys. Rev.* B **48** 11782

[38] Ossicini S, Pavesi L and Priolo F 2003 *Light Emitting Silicon for Microphotonics (Springer Tracts in Modern Physics* vol 194*)* (Berlin: Springer) p 182
[39] Markmann M, Neufeld E, Sticht A, Brunner K, Abstreiter G and Buchal C 1999 *Appl. Phys. Lett.* **75** 2584
[40] Assali L V C, Gan F, Kimerling L C and Justo J F 2003 *Appl. Phys.* A **76** 991
[41] Ostereich T, Swiatowski C and Broser I 1990 *Appl. Phys. Lett.* **56** 446
[42] Yassievich I, Bresler M and Gusev O 1998 *J. Non-Cryst. Solids* **226** 192
[43] Shin J H and Kim M J 1999 *J. Vac. Sci. Technol.* A **17** 3230
[44] Zanatta A R and Freire F L 2000 *Phys. Rev.* B **62** 2016
[45] Bresler M S, Gusev O B, Pak T E, Terukov E I, Tsendin K D and Yassievich I N 1999 *Semiconductors* **33** 622
[46] Mebratu G K, Kim M J and Shin J H 2004 *Japan. J. Appl. Phys.* **43** (1) 444
[47] Choi Y S, Sung J Y, Kim S H, Shin J H and Lee Y H 2003 *Appl. Phys. Lett.* **83** 3239
[48] Uekusa S and Inomata T 1998 *J. Lumin.* **80** 339
[49] Lombardo S, Campisano S U, van den Hoven G N and Polman A 1995 *Nucl. Instrum. Methods* B **96** 378
[50] Lombardo S and Campisano S U 1996 *Mater. Sci. Eng.* R **17** 281
[51] Kenyon A J, Trwoga P F, Federighi M and Pitt C W 1994 *J. Phys.: Condens. Matter* **6** L319
[52] Fujii M, Yoshida M, Kanzawa Y, Hayashi S and Yamamoto K 1997 *Appl. Phys. Lett.* **71** 1198
[53] Han H-K, Seo S-Y and Shin J H 2001 *Appl. Phys. Lett.* **79** 4568
[54] Wojdak M, Klik M, Forcales M, Gusev O B, Gregorkiewicz T, Pacifici D, Franzò G, Priolo F and Iacona F 2004 *Phys. Rev.* B **69** 233315
[55] Kenyon A J, Chryssou C E, Pitt C W, Shimizu-Iwayama T, Hole D E, Sharma N and Humphreys C J 2002 *J. Appl. Phys.* **91** 367
[56] Lee J, Shin J H and Park N 2005 *J. Lightwave Technol.* **23** 19
[57] Isshiki H, De Dood M J A, Polman A and Kimura T 2004 *Appl. Phys. Lett.* **85** 4343
[58] Huang M B and Ren X T 2003 *Phys. Rev.* B **68** 33203
[59] Citrin P H, Hamann D R and Northrup P A 2001 *Physica* B **308** 369
[60] Shmagin V B, Andreev B A, Morozova E N, Krasil'nik Z F, Kryzhkov D I, Kuznetsov V P, Uskova E A, Ammerlaan C A J and Pensl G 2001 *Physica* B **308** 361
[61] Priolo F, Coffa S, Franzò G, Spinella C, Carnera A and Bellani V 1993 *J. Appl. Phys.* **74** 4936
[62] Palmetshofer L, Suprun-Belevich Yu and Stepikhova M 1997 *Nucl. Instrum. Methods* B **127** 479
[63] Emtsev V V, Emtsev V V Jr, Poloskin D S, Shek E I and Sobolev N A 1999 *J. Lumin.* **80** 391
[64] Emtsev V V Jr, Poloskin D S, Shek E I, Sobolev N A and Kimerling L C 2001 *Mater. Sci. Eng.* B **81** 74
[65] Libertino S, Coffa S, Franzò G and Priolo F 1995 *J. Appl. Phys.* **78** 3867
[66] Chen Y, Chen G, Tian Y and Lu F 2002 *Semicond. Sci. Technol.* **17** 497
[67] Evans-Freeman J H, Kan P Y Y and Abdelgader N 2002 *J. Appl. Phys.* **92** 3755
[68] Widdershoven F P and Naus J P M 1989 *Mater. Sci. Eng.* B **4** 71
[69] Cavallini A, Fraboni B and Pizzini S 1998 *Appl. Phys. Lett.* **72** 468
[70] Needels M, Schluter M and Lannoo M 1993 *Phys. Rev.* B **47** 15533
[71] Terrasi A, Franzò G, Coffa S, Priolo F, D'Acapito F and Mobilio S 1997 *Appl. Phys. Lett.* **70** 1712
[72] Priolo F, Franzò G, Coffa S and Carnera A 1998 *Phys. Rev.* B **57** 4443
[73] Przybylinska H, Hendorfer G, Bruckner M, Palmetshofer L and Jantsch W 1995 *Appl. Phys. Lett.* **66** 490
[74] d'Acapito F, Mobilio S, Scalese S, Terasi A, Franzò G and Priolo F 2004 *Phys. Rev.* B **69** 153310
[75] Carey J D, Barklie R C, Donegan J F, Priolo F, Franzò G and Coffa S 1999 *Phys. Rev.* B **59** 2773
[76] Adler D L, Jacobson D C, Eaglesham D J, Marcus M A, Benton J L, Poate J M and Citrin P H 1992 *Appl. Phys. Lett.* **61** 2181
[77] Prezzi D, Eberlein T A G, Jones R, Filhol J S, Coutinho J, Shaw M J and Briddon P R 2005 *Phys. Rev.* B **71** 245203
[78] Carey J D 2002 *J. Phys.: Condens. Matter* **14** 8537
[79] Ishii M and Komukai Y 2001 *Appl. Phys. Lett.* **79** 934
[80] Ishii M and Komukai Y 2003 *J. Appl. Phys.* **94** 2368
[81] Raffa A G and Ballone P 2002 *Phys. Rev.* B **65** 121309
[82] Hashimoto M, Yanase A, Harima H and Katayama-Yoshida H 2001 *Physica* B **308** 378
[83] Wahl U, Vantomme A, De Wachter J, Moons R, Langouche G, Marques J G and Correia J G 1997 *Phys. Rev. Lett.* **79** 2069
[84] Kocher-Oberlehner G, Jantsch W, Palmetshofer L and Ulyashin A 2003 *Appl. Phys. Lett.* **83** 623
[85] Vinh N Q, Przyblinska H, Krasil'nik Z F and Gregorkiewicz T 2003 *Phys. Rev. Lett.* **90** 066401
[86] Forcales M, Gregorkiewicz T, Bresler M S, Gusev O B, Bradley I V and Wells J P R 2003 *Phys. Rev.* B **67** 085303
[87] Masterov V F, Nasredinov F S, Seregin P P, Kudoyarova V Kh, Kuznetsov A N and Terukov E I 1998 *Appl. Phys. Lett.* **72** 728
[88] Aldabergenova S B, Albrecht M, Strunk H P, Viner J, Taylor P C and Andreev A A 2001 *Mater. Sci. Eng.* B **81** 29
[89] Yassievich I N and Kimerling L C 1993 *Semicond. Sci. Technol.* **8** 718
[90] Palm J, Gan F, Zheng B, Michel J and Kimerling L C 1996 *Phys. Rev.* B **54** 17603
[91] Shin J H, van den Hoven G N and Polman A 1995 *Appl. Phys. Lett.* **67** 377
[92] Kik P G, De Dood M J A, Kikoin K and Polman A 1997 *Appl. Phys. Lett.* **70** 1721
[93] Gusev O B, Bresler M S, Pak P E, Yassievich I N, Forcales M, Vinh N Q and Gregorkiewicz T 2001 *Phys. Rev.* B **64** 75302
[94] Hamelin N, Kik P G, Suyver J F, Kikoin K, Polman A, Schönecker A and Saris F W 2000 *J. Appl. Phys.* **88** 5381
[95] Miniscalco W J 1991 *IEEE J. Lightwave Technol.* **9** 234
[96] Bresler M S, Gusev O B, Terukov E I, Yassievich I N, Zakharchenya B P, Emelyanov V I, Kamenev B P, Kashkarov P K, Konstantinova E A and Timoshenko V Yu 2001 *Mater. Sci. Eng.* B **81** 52
[97] Moskalenko A S, Yassievich I N, Forcales M, Klik M and Gregorkiewicz T 2004 *Phys. Rev.* B **70** 155201
[98] Forcales M, Gregorkiewicz T, Bresler M S, Gusev O B, Bradley I V and Wells J-P R 2003 *Phys. Rev.* B **67** 85303
[99] Yablonskiy A N, Klik M A J, Andreev B A, Kuznetsov V P, Krasilnik Z F and Gregorkiewicz T 2005 *Opt. Mater.* **27** 890
[100] Forcales M, Gregorkiewicz T, Bradley I V and Wells J-P R 2002 *Phys. Rev.* B **65** 195208
[101] Pawlak B J, Vinh N Q, Yassievich I N and Gregorkiewicz T 2001 *Phys. Rev.* B **64** 132202
[102] Coffa S, Franzò G and Priolo F 1996 *Appl. Phys. Lett.* **69** 2077
[103] Thao D T X, Ammerlaan C A J and Gregokiewicz T 2000 *J. Appl. Phys.* **88** 1443
[104] Suchocki A and Langer J M 1989 *Phys. Rev.* B **39** 7905
[105] Franzò G, Priolo F and Coffa S 1999 *J. Lumin.* **80** 19
[106] Franzò G, Coffa S, Priolo F and Spinella C 1997 *J. Appl. Phys.* **81** 2784
[107] Hangleiter A and Häcker R 1990 *Phys. Rev. Lett.* **65** 215
[108] Stimmer J, Reittinger A, Nützel J F, Holzbrecher H, Buchal Ch and Abstreiter G 1996 *Appl. Phys. Lett.* **68** 3290
[109] Jantsch W, Kocher C, Palmetshofer L, Pryzbylinska H, Stepikhova M and Preier H 2001 *Mater. Sci. Eng.* B **81** 86
[110] Ossicini S, Pavesi L and Priolo F 2003 *Light Emitting Silicon for Microphotonics (Springer Tracts in Modern Physics* vol 194*)* (Berlin: Springer) p 206

[111] Markmann M, Sticht A, Bobe F, Zandler G, Brunner K, Abstreiter G and Muller E 2002 *J. Appl. Phys.* **91** 9764
[112] Franzò G, Priolo F and Coffa S 1994 *Appl. Phys. Lett.* **64** 2235
[113] Du C X, Duteil F, Hansson G V and Ni W X 2001 *Appl. Phys. Lett.* **78** 1697
[114] Lannoo M, Delerue C and Allan G 1993 *J. Lumin.* **57** 243
[115] Canham L T 1990 *Appl. Phys. Lett.* **57** 1046
[116] Taskin T, Gardelis S, Evans J H, Hamilton B and Peaker A R 1995 *Electron. Lett.* **31** 2132
[117] Petrovich V, Volchek S, Dolgyi L, Kazuchits N, Yakovtseva V, Bondarenko V, Tsybeskov L and Fauchet P M 2000 *J. Porous Mater.* **7** 37
[118] Lopez H A and Fauchet P M 1999 *Appl. Phys. Lett.* **75** 3989
[119] Marstein E S, Skjelnes J K and Finstad T G 2002 *Phys. Scr.* T **101** 103
[120] Filippov V V, Pershukevich P P, Kuznetsova V V and Homenko V S 2002 *J. Lumin.* **99** 185
[121] Lopez H A and Fauchet P M 2001 *Mater. Sci. Eng.* B **81** 91
[122] Wu X, White R, Hommerich U, Namavar F and Cremins-Costa A M 1997 *J. Lumin.* **71** 13
[123] Suh K, Shin J H, Park O H, Bae B S, Lee J C and Choi H J 2005 *Appl. Phys. Lett.* **86** 53101
[124] Wang Z Y and Coffer J L 2004 *J. Phys. Chem.* B **108** 2497
[125] Wang W, Isshiki H, Yugo S, Saito R and Kimura T 2000 *J. Lumin.* **87** 319
[126] Wang Z Y, Li J, Huang X F, Wang L, Xu J and Chen K J 2001 *Solid State Commun.* **117** 383
[127] Zhao X W, Komuro S, Isshiki H, Aoyagi Y and Sugano T 1999 *Appl. Phys. Lett.* **74** 120
[128] Zhao X W, Isshiki H, Aoyagi Y, Sugano T and Komuro S 2000 *Mater. Sci. Eng.* B **74** 197
[129] Losurdo M, Cerqueira M F, Stepikhova M V, Alves E, Giangregorio M M, Pinto P and Ferreira J A 2001 *Physica* B **308** 374
[130] Zanatta A R 2003 *Appl. Phys. Lett.* **82** 1395
[131] Dukin A A, Feoktistov N A, Golubev V G, Medvedev A V, Pevtsov A B and Sel'kin A V 2000 *Appl. Phys. Lett.* **77** 3009
[132] Dukin A A, Feoktistov N A, Golubev V G, Medvedev A V, Pevtsov A B and Sel'kin A V 2002 *J. Non-Cryst. Solids* **299** 694
[133] Lopez H A and Fauchet P M 2000 *Appl. Phys. Lett.* **77** 3704
[134] Zhou Y, Snow P A and Russell P S 2001 *Mater. Sci. Eng.* B **81** 40
[135] Lipson M, Chen T, Chen K, Duan X and Kimerling L C 2001 *Mater. Sci. Eng.* B **81** 36
[136] Schmidt M, Zacharias M, Richter S, Fischer P, Veit P, Blasing J and Breeger B 2001 *Thin Solid Films* **397** 211
[137] Ha Y H, Kim S, Moon D W, Jhe J H and Shin J H 2001 *Appl. Phys. Lett.* **79** 287
[138] Schmidt M, Heitmann J, Scholz R and Zacharias M 2002 *J. Non-Cryst. Solids* **299** 678
[139] Zhou Y, Snow P A and Russell P St J 2000 *Appl. Phys. Lett.* **77** 2440
[140] Reece P J, Gal M, Tan H H and Jagadish C 2004 *Appl. Phys. Lett.* **85** 3363
[141] De Dood M J A, Berkhout B, Van Kats C M, Polman A and Van Blaaderen A 2002 *Chem. Mater.* **14** 2849
[142] De Dood M J A, Slooff L H, Polman A, Moroz A and Van Blaaderen A 2001 *Phys. Rev.* A **64** 033807-1
[143] DiMaria D J, Kirtley J R, Pakulis E J, Dong D W, Kuan T S, Pesavento F L, Theis T N, Cutro J A and Brorson S D 1984 *J. Appl. Phys.* **56** 401
[144] Shimizu-Iwayama T, Fujita K, Nakao S, Saitoh K, Fujita T and Itoh N 1994 *J. Appl. Phys.* **75** 7779
[145] Kenyon A J, Trwoga P F, Pitt C W and Rehm G 1996 *J. Appl. Phys.* **79** 9291
[146] Kenyon A J, Trwoga P F, Pitt C W and Rehm G 1998 *Appl. Phys. Lett.* **73** 523
[147] Shin J H, Kim M, Seo S and Lee C 1998 *Appl. Phys. Lett.* **72** 1092
[148] Franzò G, Vinciguerra V and Priolo F 1999 *Appl. Phys.* A **69** 3
[149] Zacharias M, Heitmann J, Scholz R, Kahler U, Schmidt M and Blasing J 2002 *Appl. Phys. Lett.* **80** 661
[150] Timoshenko V Y, Lisachenko M G, Shalygina O A, Kamenev B V, Zhigunov D M, Teterukov S A, Kashkarov P K, Heitmann J, Schmidt M and Zacharias M 2004 *J. Appl. Phys.* **96** 2254
[151] Kenyon A J, Chryssou C E, Pitt C W, Shimizu-Iwayama T, Hole D E, Sharma N and Humphreys C J 2001 *Mater. Sci. Eng.* B **81** 19
[152] Daldosso N *et al* 2005 *Appl. Phys. Lett.* **86** 261103
[153] Ran G Z, Chen Y, Qin W C, Fu J S, Ma Z C, Zong W H, Lu H, Qin J and Qin G G 2001 *J. Appl. Phys.* **90** 5835
[154] Chen Y, Ran G Z, Dai L, Zhang B R, Qin G G, Ma Z C and Zong W H 2002 *Appl. Phys. Lett.* **80** 2496
[155] Castagna M E, Coffa S, Monaco M, Muscara A, Carista L, Lorenti S and Messina A 2003 *Mater. Sci. Eng.* B **105** 83
[156] Wang S, Coffa S, Carius R and Buchal Ch 2001 *Mater. Sci. Eng.* B **81** 102